Available online freely at www.isisn.org

Bioscience Research

Print ISSN: 1811-9506 Online ISSN: 2218-3973

Journal by Innovative Scientific Information & Services Network

RESEARCH ARTICLE BIOSCIENCE RESEARCH, 2019 16(1):596-619. **OPEN ACCESS**

Toxicological and histopathological *in-vivo* studies for safe dose optimization of avastin and CCR2 antagonist nanoparticles

Safaa H. Mohamed[1], Soheir E. Kotob[1], Hanaa H. Ahmed[1], Ahmed A. Abd-Rabou[1*] and Mohamed S. Kishta[1]

[1]Hormones Department, Medical Research Division, National Research Centre, Dokki, Giza, **Egypt**, Affiliation ID: 60014618

***Correspondence:** ahmedchemia87@yahoo.com **Accepted:** 18 Aug.2018 **Published online:** 28 Feb. 2019

We investigate hepatic and renal toxicity caused by different doses of bevacizumab (avastin; AV) and CCR2 inhibitor (CR) in their free and nano-counterparts *in-vivo* to optimize their doses for further therapeutic applications against cancer or age-related macular degeneration. AV and CR nanoparticles were synthesized, characterized, and used for treatment for 7 groups (6 male and 6 female rats in each one) of acute toxicity experiment and another 7 groups (3 subgroups in each one; 5 male and 5 female rats in each subgroup) of chronic toxicity experiment. Histopathological, biochemical, and blood analyses were performed. The liver and kidney function levels and hematology parameters showed no significant changes of groups treated with the low doses of the AV and CR therapeutic regimens compared with control group. The light microscope showed normal glomerular and liver morphology in the groups treated with the low doses, while there were some histological changes in the high doses of the used therapies associated with some significant increased levels of GPT, GOT, ALP, serum creatinine, and urea nitrogen. AV and CR increase the risk of injury in glomerular filtration barrier and hepatocytes in a dose-dependent manner. The injury may not only associate with the rising levels of kidney and liver function tests but also with structural and morphological changes.

Keywords: Toxicity, Avastin nanoparticles, CCR2 antagonist nanoparticles, dose optimization.

INTRODUCTION

Bevacizumab, which available in the pharmaceutical market under the name of Avastin (AV), is used for treatment of many cancer types (Folkman 1971)and eye aliments The American Society of Health-System Pharmacists. (2016). AV is a monoclonal antibody used as an angiogenesis inhibitor and it slows the growth of new blood vessels through its anti-VEGF effect (Arao et al.,2011).By binding of the antibody to the VEGF, AV avoids the activation of VEGF receptor and then inhibits the angiogenesis, causing its anti-cancer effect [(Kim et al.,1993)

However, angiogenesis is the common leading cause of cancer progression, targeting the VEGF is still tricky (Bottsford et al., 2012). In the past years, injection of an anticancer drug, bevacizumab (avastin; AV), is considered as a promising anti-VEGF monoclonal antibody (Ferrara et al.,2005)

AV was listed on the World Health Organization's List of Essential Medicines (HOLEM) World Health Organization.(2015) .The wholesale cost in the developing countries is approximately $638.54 per vial International Drug Price Indicator Guide. (2016) and in the United Kingdom costs

the NHS about £242.66 British Medical Association. (2015) .Although AV is listed in the HOLEM, it causes some side effects like much other chemotherapy. For colon, lung, glioblastoma, and renal cancer treatments, the administration route is intravenous (Machado et al.,2012, Mayer 2011 and Abd-Rabou 2017)
For age-related macular degeneration, the route of administration is mainly by injection directly into the eye World Health Organization. (2013).

In cancer, administration of AV is usually associated with headache, nose bleeding, and high blood pressure. Other plain side effects may be also included, such as bleeding, gastrointestinal perforation, and allergic reactions. When AV used for age-related macular degeneration, it may cause vision loss and retinal detachment The American Society of Health-System Pharmacists. (2016)

Accordingly, dose optimization of the administrated dose of AV is very essential to minimize these burden side effects and to decrease liver and renal toxicity. One of the most commonly observed side effects caused by AV therapy is proteinuria (Izzedine et al.,2010).It elevated by a significant rate reached up to 21%-63% (Zhu et al.,2007).which is the main reason of renal toxicity-related injury (Zhao et al.,2009). Additionally, there is an evidence indicated that VEGF inhibitors may involve in podocytes poisoning (Guan et al.,2006).It was recorded that inhibition of VEGF on the glomerular endothelium may alter the endothelial surface and persuade the development of thrombotic microangiopathy (Machado et al.,2012)

It seems that, there is toxicity-related kidney dysfunction of the AV administration in high doses. However, the machineries related to the pathogenesis of kidney injury caused by AV are still obvious.

Chemokines are a superfamily plays with their receptors in many pathological procedures like cancer (Conti and Rollins 2004 and Fang et al.,2012) **.**To date, roughly fifty human chemokines have been identified. One of these chemokines is chemokine (C-C motif) ligand 2 (CCL2) which is also known as monocyte chemotactic protein-1 (MCP-1). In 1989, CCL2 was purified and cloned from human gliomas and myelomonocytic cells and was originating to participate in monocytes recruitment during inflammation and angiogenesis (Zachariae et al.,1990,Tangirala et al.,1997 and Salcedo et al.,2000).CCL2 is produced by a variety of activating cells, such as lymphocytes and macrophages (Zachariae et al.,1990)

Recent studies have reported that CCL2 is overexpressed in a majority of solid cancer types, including colon, liver, prostatic, and pancreatic cancers (Wolf et al., 2012,Zhang et al.,2010
And Monti et al.,2003). Importantly, cancer microenvironment plays a critical role in cancer progression and chemo resistance (Liu and Vunjak 2016)The crosstalk between cancer cells and the tumor-infiltrating cells is also shown as an important mediator in cancer development and resistance. For example, CCL2, which secreted by many cancer cells, mediates immune inhibitory effects and facilitates cancer metastasis, thus blocking of CCL2-CCR2 signaling by specific inhibitors or antagonists augments $CD8^+$ T-cell-mediated responses and inhibits the metastatic process (Fridlender et al.,2010 and Qian et al., 2011).Pharmacokinetic analysis of CCR2 antagonist (CR) administration revealed a short half-life (1 h). After 9 h of CR injection, it was undetectable in blood circulation. Based on single dose analysis of CR, it was suggested that a single dose every 6 h would prevent complete clearance of the drug over a day. However, authors expect the possibility of CR accumulation in the blood that may cause toxicity (Mitchell et al.,2013).Lack of chemotherapy stability in addition to the presence of adverse effects are the main obstacles led scientists to develop novel tacking approaches against cancer using nano-drug delivery that selectively kill cancer cells .(Park et al., 2008).Many delivery strategies were developed by utilizing pegylated polymeric complexation (Chae et al.,2010 and Abd-Rabou et al.,2017).Recently, we suggested that these methods increased the half-life and activity of anti-cancer agents, and reduced renal toxicity (Abd-Rabou AA et al.,2017) (Abd-Rabou et al.,2017) and (Abd-Rabou et al.,2016) .Therefore, an effective drug delivery technique needs to be industrialized to render AV and CR delivery less invasive and long-lasting. There are some nano-systems showed promise as drug delivery ones owing to their controlled and sustained release properties, subcellular size and biocompatibility with tissue and cells (Abd-Rabou et al.,2018 and Abd-Rabou et al.,2017).For AV, poly(DL-lactide-co-glycolide) (PLGA) nanoparticles was used for its delivery with release of the encapsulated AV from the nanoparticles could last four weeks life-time (Hao et al.,2009)

Pan and his companions also created long-lasting formulations (eight weeks) of AV through poly ethylene glycol (PEG)-coated PLGA

nanoparticles (Pan et al .,2011).For CR, liposome targeted nano-delivery was approached to stimulate pulmonary endothelium and prevent metastasis (Marko et al .,2015**)**

Liver function tests are essential biomarkers for hepatotoxicity caused by drugs. The glutamate pyruvate transaminase (GPT) or alanine aminotransferase (ALT) is a cellular enzyme mainly found in liver and kidney. High levels of GPT are observed in hepatic diseases and diseases of muscles and traumatisms. It is used in the diagnosis of the liver diseases. When GPT used in conjunction with aspartate aminotransferase (AST) or glutamate oxaloacetate (GOT) they aid in the diagnosis of infarcts in the myocardium, since the value of the ALT stays within the normal limits in the presence of elevated levels of AST. High concentration of GOT is found in heart muscle, liver, and skeletal muscle cells. Although an elevated level of GOT in the serum is not specific of the hepatic disease, it is used as a complementary diagnostic tool to verify the course of this disease with other enzymes like GPT and alkaline phosphatase (ALP) (Murray 1984). (Burtis et al.,1990)and(Tietz et al., 1995) ALP is an enzyme present in almost all tissues of the organism, being particularly high in liver and kidney. Both increases and decreases of serum ALP are of importance clinically, ALP elevation is an indication of obstructive liver disease, hepatitis, hepatotoxicity caused by drugs and its decrease may be a cause of vitamin C deficiency (Burtis et al.,1990,Tietz et al., 1995 and Wenger et al., 1984)

Kidney function tests are indicators of kidney effectiveness and reflect renal toxicity caused by drugs. Urea is the final result of the metabolism of proteins. Urea elevation in blood (uremia) is an indicator of renal diseases or renal obstruction (Burtis et al.,1990,Tietz et al., 1995 and, (Kaplan et al., 1984)**.**Creatinine is the result of the degradation of the creatine, component of muscles, where it can be transformed into adenosine tri-phosphate (ATP), which is a source of high energy required for the cells bioenergetics. The creatinine production depends on the modification of the muscular mass, and it varies little and the levels usually are very stable. Creatinine is excreted by the kidneys. With progressive renal insufficiency, there is retention in blood urea and creatinine. Elevate creatinine level may be indicative of renal injury (Burtis et al.,1990 andTietz et al., 1995)

Overall, we aimed, in this study, at exploring the acute and chronic toxicity of bevacizumab (avastin; AV) and CCR2 inhibitor (CR) in their free and nano-encapsulation counterparts on Wistar male and female rats. This was supplemented with biochemical and histopathological verifications, allowed us to optimize their doses for further applications used as medications against liver cancer model (Zoheir et al., 2015) and age-related macular degeneration model World Health Organization. (2013).

MATERIALS AND METHODS

Materials

Methoxy polyethylene glycol amine (mPEG-NH_2, MW 5000 Da), 1-ethyl-3-(3-dimethylaminopropyl)-carbodiimide (EDC), N-hydroxysuccinimide (NHS), heparin, polyethylene glycol (MW 5000 Da), 2-(N morpholine) ethanesulfonic acid (MES), dimethyl sulfoxide (DMSO), Tween 80, and poly L-lysine (PLL), CCR2 antagonist RS 504393: 6-Methyl-1′-[2-(5-methyl-2-phenyl-4-oxazolyl)ethyl]-spiro[4H-3,1-benzoxazine-4,4′-piperidin]-2(1H)-one(CR) were purchased from (Sigma-Aldrich, USA). Bevacizumab avastin (AV) was purchased from (Genentech Inc., USA). The GPT, GOT, ALP, urea, and creatinine diagnostic kits were purchased from (ChronoLab Systems, S.L., Barcelona, Spain). Ultrapure water (Millipore, Bedford, MA, USA) was used.

Preparation of nano-void (NV), avastin nanoparticles (AV NPs), CR nanoparticles (CR NPs), and AV-CR nanoparticles (AV-CR NPs)

According to the modified method that was recently established by the corresponding author [46], we have synthesized nano-void (NV), avastin nanoparticles (AV NPs), CR nanoparticles (CR NPs), and AV-CR nanoparticles (AV-CR NPs). To prepare PEG-exposed nanoparticles (nano-void; NV), we used a mixture of EDC and NHS. Briefly, heparin (HP: 0.1 mMol) was coupled with 0.1 mM of mPEG-NH2 (MW 5000 Da) using EDC (1.5 mMol) and NHS (1.6 mMol) in MES buffer (0.1 M, pH 5.5) at room temperature for 24 h stirring. Then, NV was prepared simply by mixing the polymer (PEG-heparin) with poly-L lysine buffer (PLL) overnight at 4^{o}C. The mix ratio (1: 6 v/v, PLL: PEG-heparin).

To prepare the PEG-nanoparticles of avastin monoclonal antibody (AV NPs), firstly the PEG-heparin polymer was synthesized as above and the core nanoparticles were prepared by mixing the polymer with PLL buffer overnight at 4^{o}C using this ratio (1:6 v/v, PLL: PEG-heparin). Then, AV

NPs were synthesized by activating the amine groups in the formed nanoparticles mixture using EDC and NHS to bind with the carboxylic groups in 25 mg/mL monoclonal antibody (AV) by stirring overnight at 4^{o}C, after that amide bonds were formed and the AV NPs were functionalized.

To prepare the PEG-nanoparticles of CCR2 antagonist RS 504393 (CR NPs), simply the PEG-heparin polymer was synthesized as above and the CR nanoparticles were prepared by mixing the polymer with PLL buffer overnight at 4oC using this ratio (1: 6 v/v, PLL: PEG-heparin). Before adding PLL to form the CR NPs, 2 mg/mL CCR2 antagonist RS 504393 of CR was titrated to the PEG/heparin polymer. This mixture was vortexed for 5 min and subsequently sonicated for 5 min using a Sonics Vibra-cell sonifier VC750 equipped with a micro-tip (Newtown, CT) at amplitude = 35%, pulse-on = 5.0 s, and pulse-off = 3.0 s. The suspension was transferred to a round-bottom tube in a water bath with magnetic stirring overnight at room temperature.

To prepare AV-CR NPs, firstly the CR NPs were synthesized as a core vehicle (as mentioned above) then the amine groups were activated using EDC and NHS to bind the carboxylic groups in 25 mg/mL monoclonal antibody (AV) by stirring overnight at 4^{o}C, after that amide bonds were formed and the AV-CR NPs were functionalized.

NPs characterization

Entrapment efficiency (EE)

All NPs were dialyzed and the concentrations were measured of the nano-conjugated AV and CR after performing dialysis tubing technique for eliminating the impurities and the free drug using a membrane bag (Spectrum Laboratories, USA; molecular weight cut-off, MWCO: 25,000 Da). The free and conjugated forms of AV and CCR2 antagonist were detected with a variable wavelength detector using UV-based ELISA system. The calibration curves for quantification of these compounds were linear over the range of standard concentrations. Finally, entrapment efficiency (EE) was calculated.

Transmission electron microscopic (TEM)

Particle morphology of all nanoparticles was examined by transmission electron microscopy (TEM, Philips CM-10, FEI Inc., Hillsboro, OR, USA). 100 µg/ml of the nano-suspensions were dropped into Formvar-coated copper grids, and after complete drying, the samples were stained using 2% w/v uranyl acetate (Electron Microscopy Services, Ft. Washington, PA). Image capture and analysis was done using Digital Micrograph and Soft Imaging Viewer Software.

Particle size distribution and zeta potential

The particle size and zeta potential analyses of all nanoparticles were performed by photon correlation spectroscopy (PCS) and laser diffractometry (LD). For PCS measurements, 1mL of the nanoparticles solution was filled in the disposable transparent sizing clear cuvette and the size of sample was analyzed at 25^{o}C with a Malvern ZetaSizer (Malvern Instruments, Westborough, Massachusetts).

***In-vivo* application**

Animals

Male and female Albino rats of Wistar strain (body weight 120 g) were used in this study. Animals were obtained from the Animal House Colony at National Research Centre, Giza, Egypt. The animals were housed in a specific pathogen free barrier area in a room with controlled temperature (22±1 ^{o}C) and humidity (50±10%) and a 12 h light/dark cycle. The rats were allowed *ad libitum* access to water and standard laboratory diet consisting of casein 10%, salts mixture 4%, vitamins mixture 1%, corn oil 10% and cellulose 5% completed to 100 g with corn starch A.O.A.C.(1995)The study protocol followed the guidelines approved by the Ethical Committee of the Medical Research of the National Research Centre (Approval No. 16/ 281).

Acute toxicity study

Forty six male and forty six female Wistar rats were enrolled in the current study and divided into 7 groups according to a single dose oral treatment(Group 1: control; Group 2: AV; Group 3: AVNP; Group 4: CR; Group 5: CRNP; Group 6: AVCR; and Group 7: AVCR NP). All groups were treated once and scarified for blood and histopathological investigations after 14 days. The groups' information was tabulated in (Table 1). We illustrated the number of experiment trails, number of rats before and after drug injection, dietary intake, and dose optimization for chronic toxicity. Each group contains 6 male and 6 female Wistar rats. We used 2 trails for each group to reach the optimum safe dose, by which we did not observe any loss in the rats number and their dietary intake is normal. This section will be mentioned in details in the results.

Chronic toxicity study

The chronic toxicity study which lasted for 2 months assesses the effect of the tested candidates which administrated orally in a daily manner over this prolonged period of time. Ninety five male and ninety five female Wistar rats were enrolled in the current study and 6 different groups (AV, AVNP, CR, CRNP, AVCR, and AVCR NP) plus control. Each group had 15 males and 15 female rats. Each group was subdivided into 3 subgroups according to the administrated dose (High dose, H; moderate dose, M; and low dose, L). Each subgroup had 5 male and 5 female rats. According to the acute toxicity results, that will be discussed latter on, we used 5 mg/kg rat as the high dose of AV and 0.001mg/kg rat as the high dose of CR. Accordingly, the H, M, and L doses of AV were 5, 2.5, and 1.25 mg/kg rat and the H, M, and L doses of CR were 0.001, 0.0005, 0.00025 mg/kg rat. We used these concentrations in both free- and nano-formulations of AV, CR, and AVCR.

Blood Sampling and Biochemical Investigations

At the end of the chronic toxicity experimental period, rats were fasted overnight and subjected to diethyl ether anesthesia. Blood samples were immediately collected from the retro-orbital venous plexus and divided into two portions, the first small portion was taken on EDTA tube (BD Company, Canada) for hematology profile analysis, while the second large portion was left to clot in clean dry test tubes, and then centrifuged at 1800 xg for ten minutes to obtain sera. The clear supernatant sera were then frozen at -20 ºC for the biochemical analyses.

Hematology profiling.

Medonic M32 analyzer included MPA micro-pipette adapter for sampling (Boule Diagnostics AB Company, Sweden) was used for hematology profiling of rat blood samples which collected using vacutainer tubes containing EDTA (BD Company, Canada). 20 µL of blood samples were collected from the vacutainer tubes and simply drawn into the micro-capillary tube connected with the MPA micro-pipette adapter for hematology profiling. Medonic M32 analyzer comes equipped with a high-precision shear-valve for getting accurate results of hematology analysis. Hematological analysis is concerned with the analysis of the cellular component of blood including tests that used for evaluation of red blood cell (RBC), hemoglobin (HGB), hematocrit (HCT), mean corpuscular volume (MCV), mean corpuscular hemoglobin (MCH), mean corpuscular hemoglobin concentration (MCHC), and red cell distribution width (RDW).

Glutamate pyruvate transaminase (GPT).

GPT catalyses the reversible transfer of an amino group from alanine to α-ketoglutarate forming glutamate and pyruvate. The pyruvate produced is reduced to lactate by lactate dehydrogenase (LDH) and NADH as shown in equations (1 and 2). The rate of decrease in concentration of NADH, measured photometrically, is proportional to the catalytic concentration of ALT present in the sample. The working reagent (WR) was prepared by mixing 4 volume R1 buffer (100 mmol/L TRIS pH 7.8, 1200 U/L lactate dehydrogenase (LDH), and 500 mmol/L L-Alanine) and 1 volume R2 Substrate (0.18 mmol/L NADH and 15 mmol/L α–Ketoglutarate) (Murray,1984).The spectrophotometer was adjusted to zero with distilled water. 1mL of the WR plus 100 µL of the serum sample was pipetted into a cuvette. They were mixed and incubated for 1 minute. The initial absorbance (A) at 340 nm of the sample was read. Using the stopwatch the absorbances at 1 minute intervals thereafter for 3 minutes were taken. The difference between absorbances and the average absorbance differences per minute (∆A/min) were calculated according the following equation (3).

L-Alanine + α -Ketoglutarate→ALT→ Glutamate + Pyruvate

------ (1)

Pyruvate + NADH + H^+→LDH→ Lactate + NAD^+------ (2)

∆A/min * 1750 = U/L GPT ------ (3)

Glutamate oxaloacetate transferase(GOT).

GOT catalyses the reversible transfer of an amino group from aspartate to α-ketoglutarate forming glutamate and oxalacetate. The oxalacetate produced is reduced to malate by malate dehydrogenase (MDH) and NADH as shown in equations (4 and 5). The rate of decrease in concentration of NADH, measured photometrically, is proportional to the catalytic concentration of GOT present in the sample [43]. The spectrophotometer was adjusted to zero with distilled water. To prepare the working reagent (WR), we have dissolved one tablet of R2 substrate (0.18 mmol/L NADH, 800 U/L Lactate dehydrogenase (LDH), 600 U/L Malate dehydrogenase (MDH), and12 mmol/L α–Ketoglutarate) with one vial of R1 buffer (80

mmol/L TRIS pH 7.8 and 200 mmol/L L-Aspartate). A mixture of 1mL of the WR and 100 µL of serum sample was added to the cuvette and mixed for 1 minute. The initial absorbance (A) at 340 nm of the sample was read, and using the stopwatch the absorbances at 1 minute intervals thereafter for 3 minutes were taken. The difference between absorbances and the average absorbance differences per minute (∆A/min) were calculated according the following equation (6).

Aspartate + α-Ketoglutarate→AST→ Glutamate + Oxalacetate ------(4)
Oxalacetate + NADH + H^+→MDH→ Malate + NAD^+------ (5)
∆A/min * 1750 = U/L of GOT ------ (6)

Alkaline phosphatase (ALP).

ALP catalyses the transfer of the phosphate group from p-nitrophenylphosphate to 2-amino-2-methyl-1-propanol (AMP), liberating p-nitrophenol according to the following equation (7). The rate of p-Nitrophenol formation, measured photometrically, is proportional to the catalytic concentration of alkaline phosphatase present in the sample [46]. To prepare the working reagent (WR), we dissolved the contents of R2 Substrate (10 mmol/L p-Nitrophenylphosphate (*p*NPP)) in the corresponding volume of R1 buffer (0.35 mol/L 2-Amino-2-methyl-1-propanol, 1 mmol/L Zinc sulfate, 2 mmol/L Magnesium acetate, and 2 mmol/L N-hydroxyethylethylenediaminetriacetic acid (EDTA)). The spectrophotometer was adjusted to zero with distilled water. A mixture of 1mL of the WR and 20 µL of serum sample was added to the cuvette and mixed for 1 minute. The initial absorbance (A) at 405 nm of the sample was read, and using the stopwatch the absorbances at 1 minute intervals thereafter for 3 minutes were taken. The difference between absorbances and the average absorbance differences per minute (∆A/min) were calculated according the following equation (8).

p-Nitrophenylphosphate + AMP →ALP→ p-Nitrophenol + Phosphate ------ (7)
∆A/min * 2764 = U/L of ALP ------ (8)

Urea.

Urea in the sample is hydrolized enzymatically into ammonia (NH_3) and carbon dioxide (CO_2). Ammonia ions formed react with α-ketoglutarate in a reaction catalysed by glutamate dehydrogenase (GLDH) with simultaneous oxidation of NADH to NAD^+ as shown in equations (9 and 10). The decrease in concentration of NADH is proportional to urea concentration in the sample1. To prepare the working reagent (WR), we dissolved the contents of R2 Enzymes (3750 U/L Urease, 6000 U/L Glutamate dehydrogenase (GLDH), and 0.32 mmol/L NADH) into the corresponding volume of R1 buffer (80 mmol/L TRIS pH 7.8 and 6 mmol/L α –Ketoglutarate) and mixed gently to dissolve contents. The spectrophotometer was adjusted to zero with distilled water. A mixture of 1mL of the WR and 10 µL of serum sample or 10 µL of standard was added to the cuvette and mixed for 1 minute. The initial absorbance (A) at 340 nm of the sample was read after 30 s (A1) and the second one after 90 s (A2). The difference between absorbances were calculated according the following equations (11 and 12).

Urea + H_2O + 2 H^+→Urease→NH_3 + CO_2------ (9)
2 NH_3 + α - Ketoglutarate + NADH →GLDH→ H_2O + NAD^+ + L-Glutamate ------ (10)
ΔA=A1–A2 ------ (11)
(ΔA Sample/ ΔA Standard) * 50 (Standard conc.) = mg/dL urea in the sample ------ (12)

Creatinine.

The assay is based on the reaction of creatinine with sodium picrate. Creatinine reacts with alkaline picrate forming a red complex. The time interval chosen for measurements avoids interferences from other serum constituents. The intensity of the color formed is proportional to the creatinine concentration in the sample1. To prepare the working reagent (WR), we mixed equal volumes of R1 (17.5 mmol/L Picric acid) and R2 Alkaline reagent (0.29 mol/L Sodium hydroxide) and mixed gently to dissolve contents. The spectrophotometer was adjusted to zero with distilled water. A mixture of 1mL of the WR and 100 µL of serum sample or 100 µL of standard was added to the cuvette and mixed for 1 minute. The initial absorbance (A) at 492 nm of the sample was read after 30 s (A1) and the second one after 90 s (A2). The difference between absorbances was calculated according the following equations (13 and 14).

ΔA= A1 – A2 ------ (13)
(ΔA Sample- ΔA Blank/ ΔA Standard- ΔA Blank) * 2 (Standard conc.)=mg/Dl creatininein the sample ------ (14)

Tissue sampling and Histopathological Investigation

After blood collection, the rats were scarified and the whole liver and kidney of each rat was rapidly dissected, thoroughly washed with isotonic saline and dried on filter paper, stored in formalin saline (10%) for histopathological investigation. After fixation of liver and kidney samples of each

rat in the different groups in 10% formalin saline for twenty four hours, washing was done in tap water. Then serial dilutions of alcohol (methyl, ethyl and absolute ethyl) were used for dehydration. Specimens were cleared in xylene and embedded in paraffin at 56ºC in hot air oven for twenty four hours. Paraffin bees wax tissue blocks were prepared for sectioning at 4 µm thickness by slidge microtome. The obtained tissue sections will be collected on glass slides, deparaffinized, and stained by hematoxylin and eosin stain. Eventually, examination was done through the light electric microscope .(Banchroft et al.,1996)

Statistical analysis

Comparisons between treated groups versus control were made using a two-tailed Student's t test, and values of $P < 0.05$ were considered statistically significant.

RESULTS

Characterization of nanoparticles

Figs. 1A-C showed the peak of the nano-void (NV) size distribution (Fig. 1A), TEM imaging (Fig. 1B), core size (109.9 nm) and shell size (161 nm) (Fig. 1C). These NV particles showed good stability with high negative charged zeta potential around -15 mV. Figs. 1D-F showed the peak of the AV NPs size distribution (Fig. 1D), TEM imaging (Fig. 1E), core size (52.3 nm) and shell size (72.02 nm) (Fig. 1F). These AV NPs showed high EE=86% and good stability with high negative charged zeta potential around -9 mV. Figs. 1G-I showed the peak of the CR NPs size distribution (Fig. 1G), TEM imaging (Fig. 1H), core size (57.7 nm) and shell size (73.3 nm) (Fig. 1I). These CR NPs showed high EE=74% and good stability with negative charged zeta potential around -3 mV. Figs. 1J-L showed the peak of the AVCR NPs size distribution (Fig. 1J), TEM imaging (Fig. 1K), core size (198.4 nm) and shell size (210 nm) (Fig. 1L). These AVCR NPs showed high EE=82% for AV and EE=75% for CR and good stability with positively charged zeta potential around 5 mV.

The calibration curves of AV and CR after dialysis tubing were performed. The serial dilutions used for drawing the AV calibration curve were as follow: 0.39, 0.78, 1.56, and 3.12 mg/mL and for the CR calibration curve were as follow: 0.0078, 0.0156, 0.0312, 0.0625, and 0.125 mg/mL.

Dose optimization based on acute toxicity study

All groups which enrolled in acute toxicity experiment were tabulated in (Table 1). We illustrated the number of experiment trails, number of rats before and after drug injection, dietary intake, and dose optimization for chronic toxicity. Briefly, 6 male and 6 female Wistar rats were used a control group (Group 1) and they were treated orally by a single dose of 0.5 mL distilled water (H_2O). Group 1 ate 100% of the supplemented food and there was no loss in their number after 14 days. So, one trail for Group 1 is sufficient. The same number of rats (6/6) was enrolled in Group 2 which was treated orally with a single dose of 5 mg/mL AV dissolved in 0.5 mL H_2O. Although there was no loss in their number after 14 days, their food intake was not completely efficient (80%). So, a second trail was mandatory to reach 100% dietary intake after oral injection of a single dose of 2.5 mg/mL AV dissolved in 0.5 mL H_2O.

The same number of rats (6/6) was enrolled in Group 3 which was treated orally with a single dose of 5 mg/mL AVNP dissolved in 0.5 mL H_2O.

Although there was no loss in their number after 14 days, their food intake was not completely efficient (70%). So, a second trail was mandatory to reach 100% dietary intake after oral injection of a single dose of 2.5 mg/mL AVNP dissolved in 0.5 mL H_2O. The same number of rats (6/6) was enrolled in Group 4 which was treated orally with a single dose of 0.1 mg/mL CR dissolved in 0.5 mL H_2O. Although there was no loss in their number after 14 days, their food intake was not completely efficient (40%). So, a second trail was mandatory to reach 100% dietary intake after oral injection of a single dose of 0.001 mg/mL CR dissolved in 0.5 mL H_2O. The same number of rats (6/6) was enrolled in Group 5 which was treated orally with a single dose of 0.1 mg/mL CRNP dissolved in 0.5 mL H_2O. We observed a loss in their number after 14 days (one from males and one from females were dead) and their food intake was not good (10%). So, a second trail was mandatory to reach 100% dietary intake after oral injection of a single dose of 0.001 mg/mL CRNP dissolved in 0.5 mL H_2O with no death. The same number of rats (6/6) was enrolled in Group 6 which was treated orally with a single dose of 5 mg/mL AV and 0.1 mg/mL CR dissolved in 0.5 mL H_2O.

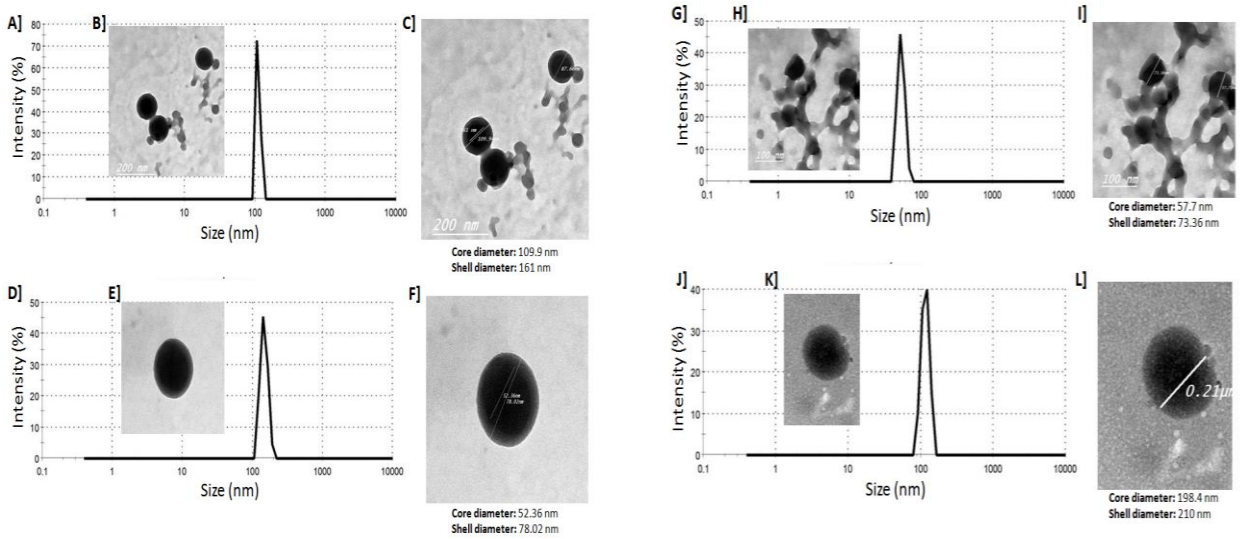

Figure. (1): AV and CR NPs characterization. A-C] the peak of the nano-void (NV) size distribution (A), TEM imaging (B), core size and shell size (C). D-F] the peak of the AV NPs size distribution (D), TEM imaging (E), core size and shell size (F). G-I] the peak of the CR NPs size distribution (G), TEM imaging (H), core size and shell size (I). J-L] the peak of the AVCR NPs size distribution (J), TEM imaging (K), core size and shell size (L).

Table (1): Acute toxicity groups, number of experiment trails, number of rats before and after drug injection, dietary intake, and dose optimization for chronic toxicity

Groups	Trail	Rat no. before injection (males/females)	Drug	Dose (mg/kg in 0.5mL H_2O)	Dietary intake (%)	Rat no. after injection (males/females)
Group 1:	1	6/6	Control (H_2O)	H_2O	100	6/6
Group 2:	1	6/6	AV	5	80	6/6
	2	6/6	AV	2.5	100	6/6
Group 3:	1	6/6	AVNP	5	70	6/6
	2	6/6	AVNP	2.5	100	6/6
Group 4:	1	6/6	CR	0.1	40	6/6
	2	6/6	CR	0.001	100	6/6
Group 5:	1	6/6	CRNP	0.1	10	5/5*
	2	6/6	CRNP	0.001	100	6/6
Group 6:	1	6/6	AVCR	5 + 0.1	30	5/6*
	2	6/6	AVCR	2.5 + 0.001	100	6/6
Group 7:	1	6/6	AVCRNP	5 + 0.1	0	1/1*
	2	6/6	AVCRNP	2.5 + 0.001	100	6/6

AV= avsatin, CR= CCR2 antagonist, NP= nanoparticles, %= percentage, H_2O= distilled water, * = death.

We observed a loss in their number after 14 days (only one from males was dead) and their food intake was not good (30%). So, a second trail was mandatory to reach 100% dietary intake after oral injection of a single dose of 2.5 mg/mL AV and 0.001 mg/mL CR dissolved in 0.5 mL H_2O with no recorded death. The same number of rats (6/6) was enrolled in Group 7 which was treated orally with a single dose of AVCRNP (5 mg/mL AV and 0.1 mg/mL CR) dissolved in 0.5 mL H_2O. We observed a dramatic loss in their number after 14 days (five from males and another five from females were dead) and their food intake was absolute zero (0%). So, a second trail was mandatory to reach 100% dietary intake after oral injection of a single dose of AVCRNP (2.5 mg/mL AV and 0.001 mg/mL CR) dissolved in 0.5 mL H_2O with no further recorded death.

Circulating glucose levels

In Fig. 2A, we have tested the glucose levels (mg/dL) circulating in rats' blood in the AV and AV NP treated groups and their subgroups depending on the drug dose (H: high, M: moderate, and L: low) versus control group. We noted that there were slight alterations between groups but within the normal ranges of the circulating glucose levels. The control's glucose level was around 90 mg/mL and non-significantly decreased ($P > 0.05$) gradually in a dose-dependent pattern after AV treatment in male and female rats from high to low doses. Oppositely, there was a significant gradual increase ($P < 0.05$) in a dose-dependent manner after AVNP treatment specifically in male rats from high to low doses.

In Fig. 2B, we have tested the glucose levels (mg/dL) circulating in rats' blood in the CR and CR NP treated groups and their subgroups depending on the drug dose (H: high, M: moderate, and L: low) versus control group. We observed that there were slight changes between groups but within the normal ranges of the circulating glucose levels. The control's glucose level was approximately 90 mg/mL and non-significantly decreased ($P > 0.05$) in a dose-dependent pattern after CR and its nano-formulation treatment specifically in male rats from high to low doses. On the other hand, there were non-significant changes ($P > 0.05$) of blood glucose levels in female rats compared to the control.

In Fig. 2C, we have tested the glucose levels (mg/dL) circulating in rats' blood in the combinatorial regimens of AVCR and its nano-particulate AVCR NP treated groups and their subgroups depending on the drug dose (H: high, M: moderate, and L: low) versus control group. We observed that there were slight changes between groups but within the normal ranges of the circulating glucose levels. The control's glucose level was approximately 90 mg/mL and non-significantly decreased ($P > 0.05$) in after AVCR treatment in male and female rats. Intriguingly, AVCR NP therapy dramatically decreased ($P < 0.01$) the blood glucose levels in male and female rats up to 50 mg/mL, with a noticed a significant dose-dependent decrease manner ($P < 0.01$) from high to low doses in the case of female rats treated with AVCR NPs.

Hematology profile

Using of Medonic M32 analyzer, rats' blood cell counted and hematological analysis was assessed, which is concerned with the analysis of the cellular component of blood including tests that used for evaluation of HGB (g/dL), MCH (pg), MCHC (g/dL), RBC (10^{12}/L), MCV (fl), HCT (%), and RDW (%). Table 2 showed the hematology profile of male and female rats treated with 3 doses (high, moderate, and low) of AV (5, 2.5, and 1.25 mg/mL rat) and CR (0.001, 0.0005, and 0.00025 mg/kg rat)-based therapeutic regimens. In the majority of the obtained results, there were non-significant changes ($P > 0.05$) observed in the treated groups and subgroups with free- and nano-AV and/or CR therapeutic regimens compared to control.

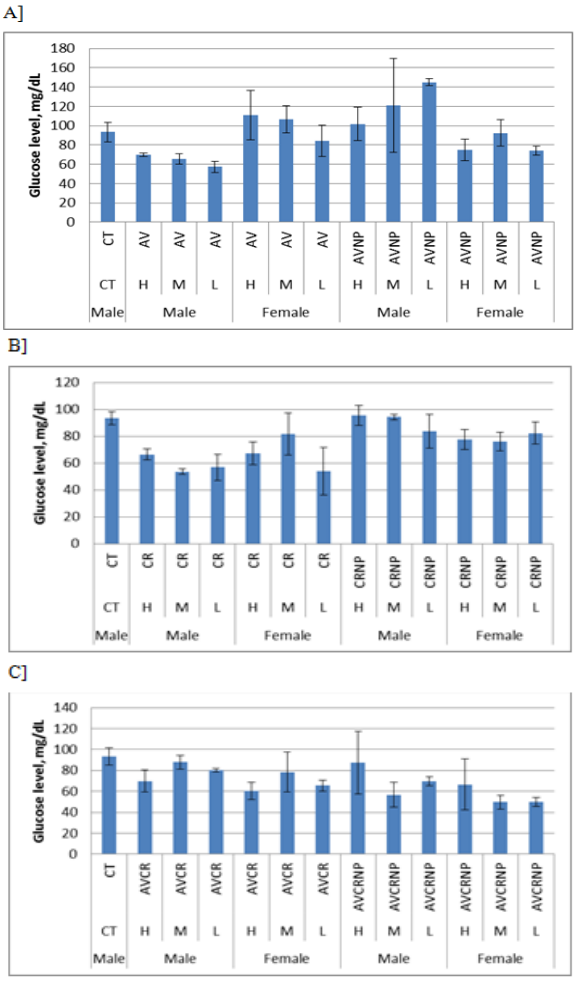

Figure. (2): Blood glucose levels in male and female rats treated with different doses (high: H, moderate: M, and low: L) of AV and CR-based therapeutic regimens.

Table (2): Hematology profile of male and female rats treated with different doses of AV and CR-based therapeutic regimens.

Sex	Dose	Group	HGB, g/dL	MCH, pg	MCHC, g/dL	RBC, 10^{12}/L	MCV, fl	HCT, %	RDW, %
Male	CT	CT	14.70	18.60	37.70	7.90	49.30	39.00	15.80
		SE	1.15	1.45	2.95	0.62	3.85	3.05	1.23
Male	High	AV	12.00	19.70	32.40	6.09	60.70	37.00	19.70
		SE	0.94	1.54	2.53	0.48	4.74	2.89	1.54
	Moderate	AV	13.10	20.10	35.60	6.52	56.40	36.80	16.50
		SE	1.02	1.57	2.78	0.51	4.41	2.88	1.29
	Low	AV	9.40*	19.50	36.20	4.82*	54.00	26.00	16.20
		SE	0.73	1.52	2.83	0.38	4.22	2.03	1.27
Female	High	AV	11.60	19.40	32.40	5.98	60.00	35.00	19.50
		SE	0.78	1.31	2.19	0.40	4.05	2.36	1.32
	Moderate	AV	13.20	19.20	36.80	6.87	52.30	36.00	15.00
		SE	1.03	1.50	2.88	0.54	4.09	2.81	1.17
	Low	AV	13.11	19.11	36.71	6.78	52.21	35.91	14.91
		SE	0.89	1.29	2.48	0.46	3.53	2.43	1.01
Male	High	AVNP	12.60	19.30	33.00	6.50	58.70	38.80	19.60
		SE	1.10	1.68	2.87	0.57	5.10	3.37	1.70
	Moderate	AVNP	12.90	19.50	32.90	6.61	59.30	39.20	16.50
		SE	0.87	1.32	2.22	0.45	4.01	2.65	1.11
	Low	AVNP	11.10	20.00	26.70*	5.55	74.60	41.40	24.00
		SE	0.97	1.74	2.32	0.48	6.49	3.60	2.09
Female	High	AVNP	14.50	20.50	36.40	7.06	56.50	39.90	15.80
		SE	1.26	1.78	3.17	0.61	4.91	3.47	1.37
	Moderate	AVNP	13.40	21.10	36.70	6.33	57.50	36.40	16.30
		SE	1.17	1.83	3.19	0.55	5.00	3.17	1.42
	Low	AVNP	13.70	20.00	35.20	6.85	56.70	38.80	14.80
		SE	1.19	1.74	3.06	0.60	4.93	3.37	1.29
Male	High	CR	11.80	20.20	34.10	5.85	59.10	34.70	15.90
		SE	1.03	1.76	2.97	0.51	5.14	3.02	1.38
	Moderate	CR	13.10	18.50	34.60	7.10	53.50	38.00	17.10
		SE	1.14	1.61	3.01	0.62	4.65	3.30	1.49
	Low	CR	12.80	19.30	36.50	6.64	52.80	35.10	15.40
		SE	1.11	1.68	3.17	0.58	4.59	3.05	1.34
Female	High	CR	12.90	20.00	32.40	6.43	61.80	39.80	21.80
		SE	1.12	1.74	2.82	0.56	5.37	3.46	1.90
	Moderate	CR	12.30	17.40	36.40	7.07	47.80	33.80	24.60
		SE	1.07	1.51	3.17	0.61	4.16	2.94	2.14
	Low	CR	12.00	20.70	36.10	5.80	57.40	33.30	17.70
		SE	1.04	1.80	3.14	0.50	4.99	2.90	1.54
Male	High	CRNP	12.30	19.20	38.70	6.42	49.70	31.90	17.70
		SE	1.07	1.67	3.37	0.56	4.32	2.77	1.54
	Moderate	CRNP	13.60	18.70	38.20	7.25	49.00	35.60	16.80
		SE	1.18	1.63	3.32	0.63	4.26	3.10	1.46
	Low	CRNP	13.90	19.10	35.30	7.26	54.20	39.40	16.40

		SE	1.21	1.66	3.07	0.63	4.71	3.43	1.43
Female	**High**	**CRNP**	12.90	19.90	35.50	6.48	56.10	36.40	17.20
		SE	1.52	2.34	4.18	0.76	6.60	4.28	2.02
	Moderate	**CRNP**	12.50	18.60	37.00	6.75	50.20	33.90	16.00
		SE	1.47	2.19	4.35	0.79	5.91	3.99	1.88
	Low	**CRNP**	12.20	19.00	37.00	6.44	51.50	33.20	16.20
		SE	1.44	2.24	4.35	0.76	6.06	3.91	1.91
Male	**High**	**AVCR**	12.60	19.30	35.20	6.51	54.90	35.80	17.00
		SE	1.48	2.27	4.14	0.77	6.46	4.21	2.00
	Moderate	**AVCR**	13.20	19.10	34.50	6.94	55.20	38.40	18.40
		SE	1.55	2.25	4.06	0.82	6.49	4.52	2.16
	Low	**AVCR**	12.50	18.20	34.70	6.87	52.40	36.00	16.90
		SE	1.47	2.14	4.08	0.81	6.16	4.24	1.99
Female	**High**	**AVCR**	12.70	18.50	36.90	6.83	50.30	34.40	16.50
		SE	1.49	2.18	4.34	0.80	5.92	4.05	1.94
	Moderate	**AVCR**	13.70	19.90	35.70	6.86	55.80	38.30	17.40
		SE	1.61	2.34	4.20	0.81	6.56	4.51	2.05
	Low	**AVCR**	14.10	19.50	35.00	7.19	55.80	40.20	16.10
		SE	1.66	2.29	4.12	0.85	6.56	4.73	1.89
Male	**High**	**AVCRNP**	12.20	20.20	34.00	6.02	59.60	35.90	18.70
		SE	1.44	2.38	4.00	0.71	7.01	4.22	2.20
	Moderate	**AVCRNP**	13.30	20.30	34.50	6.56	58.90	38.60	15.20
		SE	1.56	2.39	4.06	0.77	6.93	4.54	1.79
	Low	**AVCRNP**	12.80	18.80	33.60	6.79	56.20	38.10	21.60
		SE	1.51	2.21	3.95	0.80	6.61	4.48	2.54
Female	**High**	**AVCRNP**	16.50	19.70	37.50	8.35	52.50	43.90	15.70
		SE	1.94	2.32	4.41	0.98	6.18	5.16	1.85
	Moderate	**AVCRNP**	16.00	18.70	37.80	8.59	49.40	42.50	16.10
		SE	1.88	2.20	4.45	1.01	5.81	5.00	1.89
	Low	**AVCRNP**	13.30	18.80	38.00	7.10	49.40	35.10	15.70
		SE	1.56	2.21	4.47	0.84	5.81	4.13	1.85

AV= avsatin, CR= CCR2 antagonist, NP= nanoparticles, HBG= hemoglobin, RBC = red blood cell, MCV = mean corpuscular volume, MCH = mean corpuscular hemoglobin, MCHC = mean corpuscular hemoglobin concentration, HCT = hematocrit, RDW = red cell distribution width.

Strangely, we noticed a non-significant increase ($P > 0.05$) of the levels of HGB (g/dL), RBC (10^{12}/L), and HCT (%) in the female rats treated with high and moderate doses of AVCR NP compared to control. We recorded significant decreases ($P < 0.05$) of HGB (g/dL) and RBC (10^{12}/L) in male group treated with the low dose of AV compared with control. We observed that there was a significant decrease ($P < 0.05$) of MCHC (g/dL) in male group treated with the low dose of AVNP compared with control. In addition, there were non-significant increases ($P > 0.05$) of the levels of MCV (fl) in the female rats treated with the high dose of AV and CR, as well as in the male rats treated with the high dose of AV. Eventually, there were no significant changes in the levels of RDW (%) across the tested groups and control.

Liver function profile

We used the biochemical markers GOT, GPT, and ALP as indicators of liver status after male and female rat administration with AV, AVNP, CR, CRNP, AVCR, and AVCRNP (Table 3). High, moderate, and low doses were another factor for dose optimization procedure followed in the

current study. Male and female rats treated with high, moderate, and low doses of AV showed no significant changes ($P > 0.05$) in GOT, GPT, and ALP compared to control, except those treated with high and moderate doses of AV show significant reduction in the levels of ALP (U/L) but within the normal ranges. Male and female rats treated with high doses of AVNP showed non-significant increases in ALP (U/L) compared to control. The elevation of ALP (U/L) in those female rats was associated with GOT (U/L) levels increment. Intriguingly, there were significant increases of ALP (U/L) and GOT (U/L) in male rats treated with the high dose of CR. There were non-significant increase in the levels of GOT, GPT, and ALP (U/L) in the male rats treated with the high dose of CRNP. There was general significant reduction ($P < 0.05$) in the majority of ALP (U/L) levels in the rats treated with CRNP, AVCR, and AVCR NP, but within the normal ranges. Male and female rats treated with the high dose of AVCR showed an increase in the levels of GOT (U/L) and GPT (U/L), respectively. Intriguingly, there were non-significant increases in the GOT (U/L) and GPT (U/L) levels when male and female rats treated with the high dose of AVCR NP.

Kidney function profile

Urea and creatinine were used as supportive biomarkers for renal toxicity (Table 4). Male rats treated with the high and moderate doses of AV showed non-significant increases in urea (U/L) compared to control. Male rats treated with the high dose of CR showed non-significant increases in urea (U/L) and creatinine (U/L) compared to control. Intriguingly, there was a significant increase in the levels of creatinine (U/L) when female rats treated with the high dose of CR. In addition, there were significant increases in the levels of creatinine (U/L) when male and female rats treated with the high dose of CRNP, while non-significant increase in urea (U/L) when male rats treated with CRNP. Intriguingly, there was a significant increase in the levels of creatinine (U/L) when male rats treated with the high dose of AVCR, while non-significant increase in urea (U/L) when male rats treated with AVCR. We also found that there was a significant increase in the levels of creatinine (U/L) when female rats treated with the high dose of AVCR NP, while non-significant increase in the levels of creatinine (U/L) when male rats treated with the same nano-platform.

Table (3): Liver function profile of male and female rats treated with different doses of AV and CR-based therapeutic regimens.

Sex	Dose	Group	GOT, U/L		GPT, U/L		ALP, U/L	
			Mean	SE	Mean	SE	Mean	SE
Male	**CT**	**CT**	50.73	5.47	43.19	14.69	114.65	8.36
Male	**High**	**AV**	39.2	9.76	8.08	4.52	60.46*	13.51
	Moderate	**AV**	50.83	10.30	8.75	5.05	56.12*	15.41
	Low	**AV**	48.13	12.69	12.62	11.23	112.41	42.87
Female	**High**	**AV**	37.83	8.22	17.6	1.60	101.92	26.28
	Moderate	**AV**	41.2	7.11	24.69	4.18	135.18	32.67
	Low	**AV**	30.89	5.83	13.07	5.90	139.24	22.61
Male	**High**	**AVNP**	35.1	10.86	17.39	5.99	170.79	36.16
	Moderate	**AVNP**	54.48	4.96	17.25	0.25	150.67	26.03
	Low	**AVNP**	38.98	10.36	14.55	5.85	100.03	31.17
Female	**High**	**AVNP**	65.11	0.49	14.88	1.75	159.23	20.05
	Moderate	**AVNP**	54.24	6.14	24.97	3.39	92.02	52.79
	Low	**AVNP**	53.75	4.46	38.77	16.19	121.43	30.08
Male	**High**	**CR**	91.59*	4.87	24.69	10.31	226.37*	37.80
	Moderate	**CR**	47.57	5.85	24.22	4.63	114.99	42.48
	Low	**CR**	46.67	5.04	23.61	8.91	97.04	48.80
Female	**High**	**CR**	61.12	11.63	16.8	8.14	74.83	48.59
	Moderate	**CR**	49.96	15.28	15.15	5.58	99.53	8.26

	Low	**CR**	48.21	5.28	11.04	9.16	81.45	22.33
Male	**High**	**CRNP**	68.04	34.71	64.65	2.44	124.93	18.80
	Moderate	**CRNP**	56.28	12.31	59.19	1.97	76.1	27.35
	Low	**CRNP**	52.03	8.05	14.4	5.81	59.93*	7.05
Female	**High**	**CRNP**	35.62	2.85	26	15.51	42.56*	2.77
	Moderate	**CRNP**	38.9	9.21	21.47	10.84	59.1*	19.44
	Low	**CRNP**	46.51	14.06	28.51	9.97	47.95*	7.53
Male	**High**	**AVCR**	74	17.64	31.8	4.76	57.97*	7.40
	Moderate	**AVCR**	19.91	3.76	12.33	5.80	32.55*	6.82
	Low	**AVCR**	49.34	6.89	22.17	4.21	29.39*	12.23
Female	**High**	**AVCR**	23.04	14.62	71.86	9.92	31.22*	19.61
	Moderate	**AVCR**	46.07	3.46	17.13	2.10	188.14	58.53
	Low	**AVCR**	16.1*	3.02	19.63	1.00	29.9*	3.00
Male	**High**	**AVCRNP**	65.01	10.38	61.6	6.50	112.73	6.73
	Moderate	**AVCRNP**	47.04	24.79	26.69	1.02	125.42	81.19
	Low	**AVCRNP**	19.54*	2.03	29.75	3.00	25.8*	2.00
Female	**High**	**AVCRNP**	62.23	2.79	70.06	2.95	14.8*	8.34
	Moderate	**AVCRNP**	44.96	10.30	22.49	16.93	44.08*	8.67
	Low	**AVCRNP**	44.14	12.07	10.97	3.21	91.12	5.49

Table (4): Kidney function profile of male and female rats treated with different doses of AV and CR-based therapeutic regimens.

Sex	**Dose**	**Group**	**Urea, U/L**		**Creatinine, U/L**	
			Mean	**SE**	**Mean**	**SE**
Male	**CT**	**CT**	10.86	3.44	0.99	0.39
Male	**High**	**AV**	17.42	1.82	1.24	0.18
	Moderate	**AV**	16.44	0.36	1.04	0.16
	Low	**AV**	11.12	0.11	0.90	0.10
Female	**High**	**AV**	11.81	0.98	0.75	0.20
	Moderate	**AV**	13.76	1.57	1.03	0.12
	Low	**AV**	14.76	1.06	0.82	0.10
Male	**High**	**AVNP**	11.89	1.07	1.22	0.15
	Moderate	**AVNP**	17.21	1.34	1.10	0.11
	Low	**AVNP**	15.76	2.30	0.78	0.14
Female	**High**	**AVNP**	13.54	0.95	1.62	0.44
	Moderate	**AVNP**	12.69	0.98	1.08	0.02
	Low	**AVNP**	13.04	1.33	1.08	0.18
Male	**High**	**CR**	16.48	0.66	1.75	0.43
	Moderate	**CR**	11.43	3.35	1.07	0.06
	Low	**CR**	13.58	1.96	0.86	0.12
Female	**High**	**CR**	12.20	0.65	2.22*	0.15
	Moderate	**CR**	14.11	1.33	1.24	0.15
	Low	**CR**	15.41	1.02	0.65	0.13
Male	**High**	**CRNP**	18.56	1.64	4.14*	0.23
	Moderate	**CRNP**	14.58	2.49	1.05	0.16

	Low	**CRNP**	12.87	2.67	0.66	0.10
Female	**High**	**CRNP**	15.35	2.64	2.56*	0.10
	Moderate	**CRNP**	14.81	0.63	0.75	0.07
	Low	**CRNP**	16.57	1.07	0.83	2.11
Male	**High**	**AVCR**	16.50	2.30	2.61*	0.82
	Moderate	**AVCR**	15.24	0.23	1.58	0.88
	Low	**AVCR**	15.39	2.34	1.80	0.81
Female	**High**	**AVCR**	14.10	1.11	1.87	1.37
	Moderate	**AVCR**	12.99	1.13	1.26	0.96
	Low	**AVCR**	10.18	0.00	1.04	0.00
Male	**High**	**AVCRNP**	10.88	0.59	2.28	0.70
	Moderate	**AVCRNP**	8.80	0.98	0.73	0.43
	Low	**AVCRNP**	6.42	0.81	0.50	0.00
Female	**High**	**AVCRNP**	13.46	3.03	3.38*	0.08
	Moderate	**AVCRNP**	15.21	1.71	1.10	0.57
	Low	**AVCRNP**	13.27	0.65	1.35	0.22

Histopathological profile

The obtained tissue sections taken from the rat liver were stained by hematoxylin and eosin stains for examination through the light electric microscope. Histopathological alterations were showed in (Fig. 3).

Fig. 3A showed group of control versus male rats treated with AV. *Control liver:* There was no histopathological alteration and the normal histological structure of the central vein and surrounding hepatocytes in the parenchyma were recorded. *Control kidney:* There was no histopathological alteration and the normal histological structure of the glomeruli and tubules at the cortex were recorded. *Male rats treated with AV: Liver with high dose of AV:* Focal necrosis was detected in the parenchyma while the portal area showed inflammatory cells infiltration. *Kidney with high dose of AV:* Congestion was detected in the cortical blood vessels. *Liver with moderate dose of AV:* The portal area showed few inflammatory cells infiltration while the parenchyma had focal necrosis. *Kidney with moderate dose of AV*: There was no histopathological alteration. *Liver with low dose of AV:* The parenchyma showed focal necrosis with inflammatory cells infiltration associated with congestion in the central vein. *Kidney with low dose of AV:* Congestion was observed in the cortical blood vessels.

Fig. 3B showed group of female rats treated with AV. *Liver with high dose of AV*: The portal area showed congestion in the portal vein with oedema and periductal fibrosis surrounding the bile ducts. *Kidney with high dose of AV:* There was no histopathological alteration. *Liver with moderate dose of AV:* The portal area showed inflammatory cells. *Kidney with moderate dose of AV*: There was no histopathological alteration. *Liver with low dose of AV:* Focal necrosis with inflammatory cells infiltration was detected in the parenchyma associated with oedema and inflammatory cells infiltration in the portal area. *Kidney with low dose of AV:* There was no histopathological alteration.

Fig. 3C showed group of male rats treated with AVNP. *Liver with high dose of AVNP*: The parenchyma showed focal necrosis associated with inflammatory cells infiltration in the portal area. *Kidney with high dose of AVNP*: There was congestion in the cortical blood vessels. *Liver with moderate dose of AVNP*: The parenchyma showed focal inflammatory cells aggregation. *Kidney with moderate dose of AVNP*: There was no histopathological alteration. *Liver with low dose of AVNP:* Focal necroses with inflammatory cells infiltration were detected in the parenchyma. *Kidney with low dose of AVNP:* There was no histopathological alteration.

Fig. 3D showed group of female rats treated with AVNP. *Liver with high dose of AVNP*: Focal inflammatory cells aggregation was detected in the parenchyma. *Kidney with high dose of AVNP*: There was no histopathological alteration. *Liver with moderate dose of AVNP*: The portal area showed inflammatory cells infiltration while the parenchyma had focal necrosis. *Kidney with moderate dose of AVNP*: There was no

histopathological alteration. *Liver with low dose of AVNP:* There was no histopathological alteration. *Kidney with low dose of AVNP:* There was no histopathological alteration.

Fig. 3E showed group of male rats treated with CR: *Liver with high dose of CR:* The portal area showed few inflammatory cells infiltration. *Kidney with high dose of CR*: There were focal haemorrhages in the corticomedullary portion. *Liver with moderate dose of CR:* There was congestion in the portal vein. *Kidney with moderate dose of CR*: There was no histopathological alteration. *Liver with low dose of CR:* Inflammatory cells infiltration was detected in the portal area. *Kidney with low dose of CR:* There was congestion in the cortical blood vessels.

Fig. 3F showed group of female rats treated with CR: *Liver with high dose of CR:* The portal area showed massive inflammatory cells infiltration associated with focal necrosis in the parenchyma. *Kidney with high dose of CR*: The cortex showed congestion in the blood capillaries and glomeruli with degeneration in the tubular lining epithelium. *Liver with moderate dose of CR*: The portal area showed massive inflammatory cells infiltration as well as focal inflammatory cells aggregation in the parenchyma. *Kidney with moderate dose of CR*: There was perivascular inflammatory cells aggregation associated with tubular degeneration. *Liver with low dose of CR*: Inflammatory cells infiltration was detected in the portal area. *Kidney with low dose of CR:* There was congestion in the cortical blood vessels while the corticomedullary portion showed focal haemorrhages in between the degenerated tubules.

Fig. 3G showed group of male rats treated with CRNP: *Liver with high dose of CRNP:* Massive inflammatory cells infiltration was detected in the portal area. *Kidney with high dose of CRNP*: Sever congestion was observed in the cortical blood vessels. *Liver with moderate dose of CRNP*: There were oedema and congestion in the portal vein at the portal area associated with periductal fibrosis surrounding the bile ducts. *Kidney with moderate dose of CRNP*: The glomeruli were congested while the tubules showed degeneration in the lining epithelium at the cortex. *Liver with low dose of CRNP*: The portal area showed focal inflammatory cells aggregation as well as diffuses inflammatory cells infiltration in the others with congestion in the portal vein. *Kidney with low dose of CRNP*: There was congestion in the glomeruli and degeneration in the lining epithelium of the cortical blood vessels.

Fig. 3H showed group of female rats treated with CRNP: *Liver with high dose of CRNP:* Periductal fibrosis with inflammatory cells infiltration was detected surrounding the bile ducts at the portal area with congestion in the portal vein. *Kidney with high dose of CRNP*: The cortex showed degeneration in the lining epithelium of the tubules. *Liver with moderate dose of CRNP*: Oedema with few inflammatory cells infiltration was detected in the portal area associated with congestion in the portal vein as well as periductal fibrosis surrounding the bile ducts. *Kidney with moderate dose of CRNP*: There was degenerative change in the tubular lining epithelium of the cortex. *Liver with low dose of CRNP*: The portal area showed inflammatory cells infiltration. *Kidney with low dose of CRNP*: Congestion was detected in the cortical blood vessels.

Fig. 3I showed group of male rats treated with AVCR: *Liver with high dose of AVCR:* The portal area showed inflammatory cells infiltration. *Kidney with high dose of AVCR*: There was no histopathological alteration. *Liver with moderate dose of AVCR:* There was focal necrosis in the hepatic parenchyma. *Kidney with moderate dose of AVCR:* There was no histopathological alteration. *Liver with low dose of AVCR*: The portal area showed inflammatory cells infiltration. *Kidney with low dose of AVCR:* There was degeneration in the tubular lining epithelium at the cortex.

Fig. 3J showed group of female rats treated with AVCR: *Liver with high dose of AVCR:* The portal area showed inflammatory cells infiltration associated with congestion in the portal vein and hyperplasia in the bile ducts. *Kidney with high dose of AVCR*: The tubule at the cortex showed degenerative change in the lining epithelium. *Liver with moderate dose of AVCR:* The portal area showed fibrosis, inflammatory cells infiltration and hyperplasia in the bile ducts. *Kidney with moderate dose of AVCR*: There was no histopathological alteration. *Liver with low dose of AVCR*: Few inflammatory cells infiltration was detected in the portal area associated with fatty change in the adjacent surrounding hepatocytes. *Kidney with low dose of AVCR:* There was no histopathological alteration.

Fig. 3K showed group of male rats treated with AVCRNP: *Liver with high dose of AVCRNP:* Massive inflammatory cells infiltration was detected in the portal area.

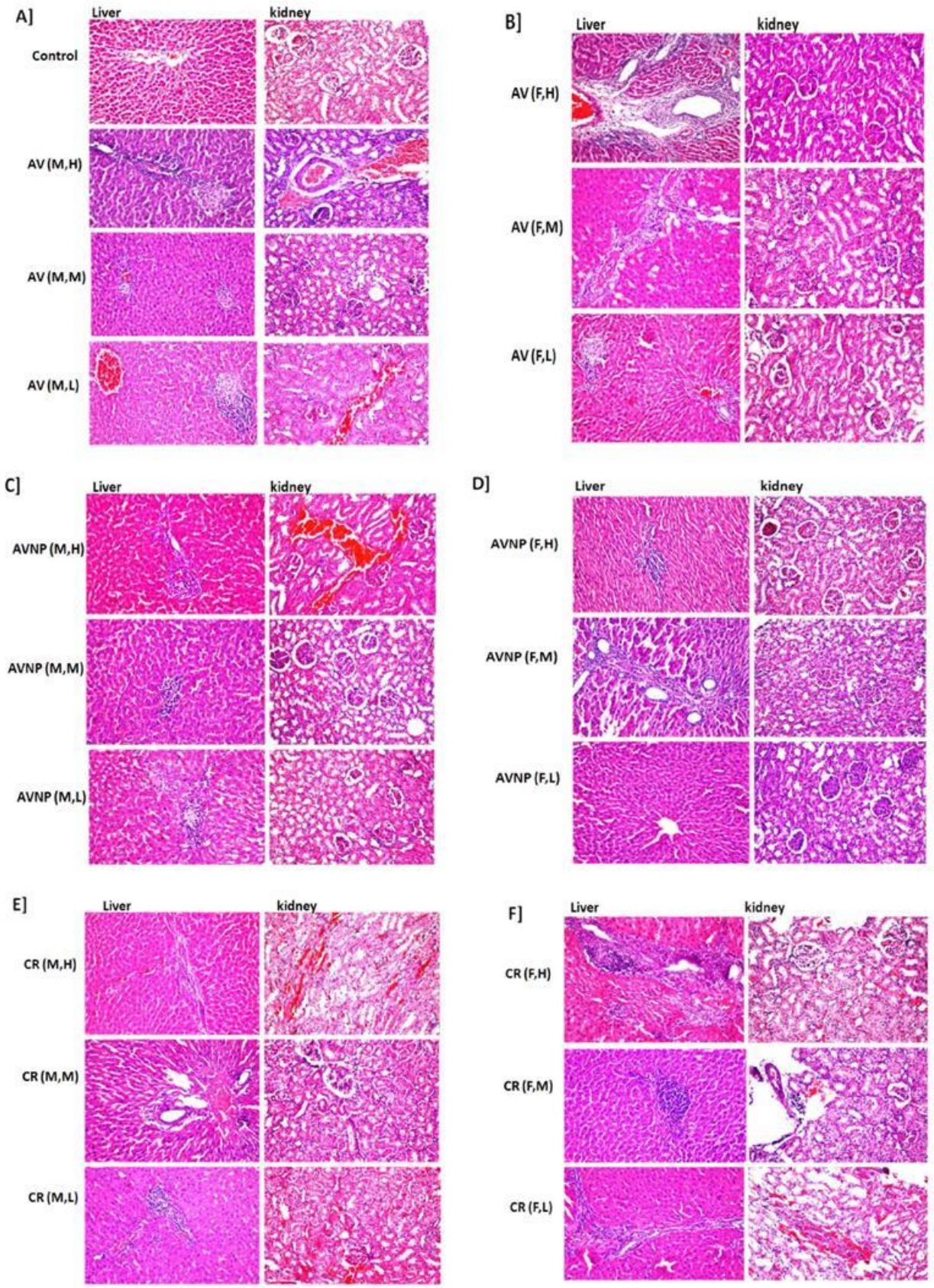
A]
Liver
kidney
Control
AV (M,H)
AV (M,M)
AV (M,L)
B]
Liver
kidney
AV (F,H)
AV (F,M)
AV (F,L)
C]
Liver
kidney
AVNP (M,H)
AVNP (M,M)
AVNP (M,L)
D]
Liver
kidney
AVNP (F,H)
AVNP (F,M)
AVNP (F,L)
E]
Liver
kidney
CR (M,H)
CR (M,M)
CR (M,L)
F]
Liver
kidney
CR (F,H)
CR (F,M)
CR (F,L)

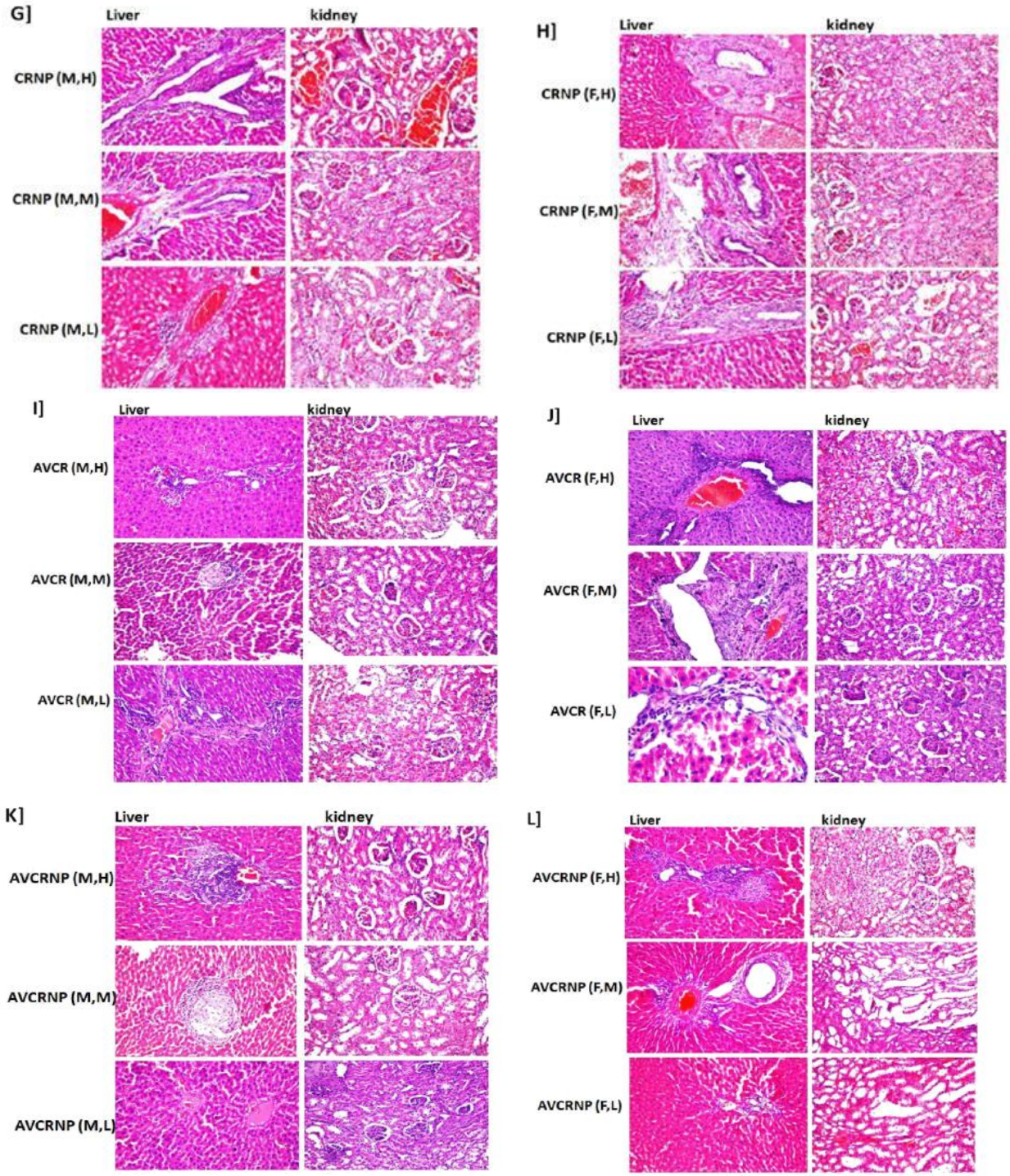
G]
Liver
kidney
CRNP (M,H)
CRNP (M,M)
CRNP (M,L)
H]
Liver
kidney
CRNP (F,H)
CRNP (F,M)
CRNP (F,L)
I]
Liver
kidney
AVCR (M,H)
AVCR (M,M)
AVCR (M,L)
J]
Liver
kidney
AVCR (F,H)
AVCR (F,M)
AVCR (F,L)
K]
Liver
kidney
AVCRNP (M,H)
AVCRNP (M,M)
AVCRNP (M,L)
L]
Liver
kidney
AVCRNP (F,H)
AVCRNP (F,M)
AVCRNP (F,L)

Kidney with high dose of AVCRNP: There was no histopathological alteration. *Liver with moderate dose of AVCRNP:* Focal necrosis was detected in the parenchyma while the portal area showed inflammatory cells infiltration. *Kidney with moderate dose of AVCRNP*: There was no histopathological alteration. *Liver with low dose of AVCRNP:* There was no histopathological alteration. *Kidney with low dose of AVCRNP*: There was no histopathological alteration.

Fig. 3L showed group of female rats treated with AVCRNP: *Liver with high dose of AVCRNP:* Focal necrosis was noticed in the parenchyma while the portal area showed inflammatory cells infiltration. *Kidney with high dose of AVCRNP:* The cortex showed **Fig. (3): Histopathological investigations. A] Group of control versus male rats treated with AV.** Control liver, Control kidney, AV (M, H)= Male rats treated with AV; Liver with high dose of AV and Kidney with high dose of AV. AV (M, M)=Liver with moderate dose of AV and Kidney with moderate dose of AV. AV (M, L)= Liver with low dose of AV and Kidney with low dose of AV. **B]**

Group of female rats treated with AV. AV (F, H)=Liver with high dose of AV and Kidney with high dose of AV. AV (F, M)= Liver with moderate dose of AV and Kidney with moderate dose of AV. AV (F, L)= Liver with low dose of AV and Kidney with low dose of AV.**C] Group of male rats treated with AVNP.** AVNP (M, H)=Liver with high dose of AVNP and Kidney with high dose of AVNP and Kidney with moderate dose of AVNP. AVNP (M, L)=Liver with low dose of AVNP and Kidney with low dose of AVNP.**D] Group of female rats treated with AVNP.** AVNP (F, H)=Liver with high dose of AVNP and Kidney with high dose of AVNP. AVNP (F, M)= Liver with moderate dose of AVNP and Kidney with moderate dose of AVNP. AVNP (F, L)= Liver with low dose of AVNP and Kidney with low dose of AVNP: **E] Group of male rats treated with CR**: CR (M, H)= Liver with high dose of CR and Kidney with high dose of CR. CR (M, M)= Liver with moderate dose of CR and Kidney with moderate dose of CR. CR (M, L)= Liver with low dose of CR and Kidney with low dose of CR. **F] Group of female rats treated with CR**: CR (F, H)= Liver with high dose of CR and Kidney with high dose of CR. CR (F, M)= Liver with moderate dose of CR and Kidney with moderate dose of CR. CR (F, L)= Liver with low dose of CR and Kidney with low dose of CR. **G] Group of male rats treated with CRNP**: CRNP (M, H)= Liver with high dose of CRNP and Kidney with high dose of CRNP. CRNP (M, M)= Liver with moderate dose of CRNP and Kidney with moderate dose of CRNP. CRNP (M, L)= Liver with low dose of CRNP and Kidney with low dose of CRNP. **H] Group of female rats treated with CRNP**: CRNP (F, H)= Liver with high dose of CRNP and Kidney with high dose of CRNP. CRNP (F, M)= Liver with moderate dose of CRNP and Kidney with moderate dose of CRNP. CRNP (F, L)= Liver with low dose of CRNP and Kidney with low dose of CRNP. **I] Group of male rats treated with AVCR**: AVCR (M, H)= Liver with high dose of AVCR and Kidney with high dose of AVCR. AVCR (M, M)= Liver with moderate dose of AVCR and Kidney with moderate dose of AVCR. AVCR (M, L)= Liver with low dose of AVCR and Kidney with low dose of AVCR. **J] Group of female rats treated with AVCR**: AVCR (F, H)= Liver with high dose of AVCR and Kidney with high dose of AVCR. AVCR (F, M)= Liver with moderate dose of AVCR and Kidney with moderate dose of AVCR. AVCR (F, L)= Liver with low dose of AVCR and Kidney with low dose of AVCR. **K] Group of male rats treated with AVCRNP:** AVCRNP (M, H)= Liver with high dose of AVCRNP and Kidney with high dose of AVCRNP. AVCRNP (M, M)= Liver with moderate dose of AVCRNP and Kidney with moderate dose of AVCRNP. AVCRNP (M, L)= Liver with low dose of AVCRNP and Kidney with low dose of AVCRNP. **L] Group of female rats treated with AVCRNP:** AVCRNP (F, H)= Liver with high dose of AVCRNP and Kidney with high dose of AVCRNP. AVCRNP (F, M)=Liver with moderate dose of AVCRNP and Kidney with high dose of AVCRNP. AVCRNP (F, L)=Liver with low dose of AVCRNP and Kidney with low dose of AVCRNP.

DISCUSSION

However, the usefulness of avastin (AV) **(** Folkman J. 1971 and (Kim et al.,1993). and CCR2 antagonist (CR) (Tangirala et al.,1997) (Zachariae et al.,1990)and (Salcedo et al.,2000) as anti-cancer agents have been reported, there are evidences also proved their burden side effects including toxicity of AV (Machado et al.,2012 ,Mayer 2011 and (Abd-Rabou 2017) and CR **(** Mitchell et al.,2013). Thus, polymeric nano-drug delivery approaches were followed to increase the half-life and activity of these anti-cancer agents, and reduced renal toxicity [(Abd-Rabou and Edris 2017) ,(Abd-Rabou et al.,2017)and (Abd-Rabou et al.,2016) **.**Dose optimization of the administrated dose of AV and CR is also very mandatory to minimize the burden side effects and to decrease liver and renal toxicity.

In the present study, we designed, synthesized, and characterized AV and CR NPs based on the knowledge of polyethylene glycol (PEG) polymeric nano-formulation, to test their toxic efficacy on the liver and the kidney of the enrolled rats, allowing us to optimize their concentrations in the free forms and their nano-counterparts. We used PEG and poly-l-lysine (PLL) for synthesizing the AV, CR, and AVCR NPs. Poly-l-lysine (PLL) has an advantage of being hydrodegradable, biodegradable, and biocompatible [49], and so it is suitable for the backbone as a drug delivery carrier. It has been reported that PLL-modified poly (lactic-co-glycolic acid) (PLGA) NPs showed significantly higher entrapment efficiency (EE%) than PLGA NPs (Tahara et al.,2010)

PLGA, when combined with PLL and PEG, has a relatively rapid rate of hydrolysis and it could reduce systemic clearance rates and prolong circulation half-life (Bao et al.,2015).Therefore, we selected PLL and PEG for encapsulating AV and CR to achieve high bioavailability and biocompatibility.

Authors found that PLGA-PLL-PEG NPs are considered as an efficient drug delivery system (Bao et al.,2015).The latter observation is in parallel with our results regarding AV and/or CR-loaded PEG-PLL NPs showed promising nano-drug delivery approach *in vivo*. In the previous reported studies, authors used PLGA-based NPs for anti-VEGF inhibitor (ganciclovir .(Duvvuri et al.,2007)

and dexamethasone acetate (Xu et al., 2007).encapsulation, and they neither reported toxicity signs nor significant inflammatory responses for periods of up to two months [54]. In parallel, we used PEG-PLL NPs for anti-VEGF inhibitor (AV) encapsulation and we did not observe liver or kidney toxicity at its low concentration.

Our AV PEG-PLL NPs noted high entrapment efficiency (EE= 86%) of AV with high stability and the particles did not lost its uniformity over 6 months based on the zeta potential negative charges (-9.00) reported on the surface of the synthesized NPs, then z-average diameter came to confirm that it is in the nano-range (core size = 52.3 nm and shell size = 72.02 nm). These observed results were in agreement with a previous study [64] indicated that the synthesized AV PLGA NPs had a slightly higher loading of AV (EE= 90%) compared to our NPs (EE= 86%), but in their case the PLGA particles lost its uniformity, this was most likely owing to partial phase separation of PLGA polymer and AV. When authors added PEG to their NPs (PEG-PLGA), the new NPs were long-circulating. This is due to, unlike PLGA, PEG is hydrophilic and retains water. The hydrophilicity of PEG also facilitated dispensing the particles compared to PLGA. This resulted in a lower yield of the particles as the majority of the polymer was dissolved in the water phase during particle preparation (Li et al ., 2012).These results are confirming the advantage of our usage for PEG plus PLL instead of PLGA in the current study.

On the other hand, another team encapsulated AV using PLGA NPs and the EE was lower than ours by 41% (i.e. EE = 45%). The release of the encapsulated AV from the NPs could last four weeks life-time (Hao et al.,2009).Pan and his companions also created long-lasting formulations (eight weeks) of AV through PEG-coated PLGA nanoparticles (Pan et al .,2011)

Authors tested a nano-based micelles approach for a targeted delivery of the CR to metastatic sites in lung. Blocking of CCR2 resulted in reduced induction of the lungs vascular permeability, and thereby reduced tumor cell extravasation. They concluded that CCR2 signaling inhibition represents a potential anti-cancer treatment without affecting homeostatic functions (Marko et al .,2015).The latter finding is in agreement with our synthesized CRNP which had potential nano-characteristics (core size= 57.7 nm, shell size= 73.3 nm, EE= 74%, zeta potential= -3 mV), allowing it to target CCR2 signaling pathway *in-vivo*. When we synthesized a nano-combinatorial form of AV and CR (AVCR NP), we resulted in a novel nano-platform with special characteristics (core size =198.4 nm, shell size = 210 nm, EE= 82% for AV, EE=75% for CR, and zeta potential = 5 mV).

Authors used cisplatin as a comparative drug to show the effect of AV on nephrotoxicity *in-vivo*, because cisplatin is an antineoplastic drug like AV and used in the treatment of various cancers (lung (Baty et al.,2013) ovarian (Sato and Itamochi 2012)etc), which also bring dose-limiting side effect such as nephrotoxicity (Aleksunes et al.,2008).They used cisplatin as because its continuous doses was commonly used in inducing rat kidney failure model (Singh et al.,2012) .They used high (5 mg/kg) and low (2.5 mg/kg) doses of AV for that purpose. In the current study, we investigated the kidney and liver functions and pathology effects on administration of different doses of AV(high 5 mg/kg, moderate 2.5 mg/kg,

and low 1.25 mg/kg) treated rats and untreated rats up to 8 weeks, trying to uncover the mechanisms involving in kidney and liver injury. The results will be beneficial for rational use in clinical therapy.

Given the fact that VEGF inhibitor displays clinically side effect in many cancer therapies (Pellé et al., 2011).we wished to reveal the toxicity mechanism of AV and CR in their free and nano-formulations on kidney and liver injury by administrated with the three mentioned dose. Our study demonstrated that AV therapy remarkably increased urea levels in rats treated with the high dose of AV, while urea and creatinine were significantly elevated in rats treated with the high doses of all CR-based regimens (i.e. CR, CRNP, AVCR, and AVCRNP) compared with control group rats. We noticed that the ranges of blood urea and creatinine back to normal at the low doses of all treatments. Our results are in parallel with a previous study (Ning et al., 2014).indicated that rat therapy with the high dose of AV statistically increased the urea nitrogen and serum creatinine levels compared with control group rats. They added that there was a significant increase in proteinuria as well, which reflects toxicity at the high dose of AV. In addition, authors suggested that the continuous dosing of CR may cause toxicity (Mitchell et al.,2013)

Clinically-wise, early kidney injury is characterized by a rapid decline of glomerular filtration rate and sudden loss of kidney function, and clinically detected by an increase in serum creatinine and urea (Hu et al ., 2012) .In our study, both of the serum creatinine and urea nitrogen were detected increased in all the high doses of AV and CR-based groups, indicating a kidney injury occurred in these rats after giving these drugs, while the urea nitrogen and serum creatinine significant increase was not reported in the low doses-treated groups. These results are in agreement with a previous study (Ning et al., 2014).Previous results proved that creatinine did not accurately estimate the glomerular filtration rate attributing to the secretion and reabsorption of kidney tubule (Bellomo et al ., 2004) .Compared with serum creatinine and blood urea nitrogen, authors showed microalbumin and cystatin C levels were more sensitive for early kidney injury detection because a more significantly dose dependent increase was found in these treatments (Ning et al., 2014).These results were in coincidence with previous studies that microalbumin and cystatin C were considered to be the more promising and easier measurable markers for the progression of kidney injury (Herget et al ., 2004).

Generally, we found observed that rats treated with high, moderate, and low doses of AV showed no significant increases (P**>** 0.05) in GOT, GPT, and ALP compared to control, except some reported cases. (1) Rats treated with high doses of AVNP showed non-significant increases in ALP compared to control. The elevation of ALP in those female rats was associated with GOT (U/L) levels increment. (2) There were significant increases of ALP and GOT in male rats treated with the high dose of CR. There were non-significant increase in the levels of GOT, GPT, and ALP in the male rats treated with the high dose of CRNP. (3) Rats treated with the high dose of AVCR showed an increase in the levels of GOT and GPT, respectively. (4) There were non-significant increases in the GOT and GPT levels when male and female rats treated with the high dose of AVCR NP.

Hematological analysis showed non-significant increases in the treated groups and subgroups with free- and nano-AV and/or CR therapeutic regimens compared with control. Except, we noticed a non-significant increase of the levels of HGB (g/dL), RBC (10^{12}/L), and HCT (%) in the female rats treated with high and moderate doses of AVCR NP compared to control. Therefore, we strongly recommend that kidney and liver functions plus hematology profile should be carefully detected in patients who were treated with AV and CR for cancer diseases, even without clinical signs.

In this study, histopathological images showed some changes, especially in the high doses of AV and CR, such as focal necrosis in the parenchyma while the portal area showed inflammatory cells infiltration in liver and congestion in the cortical blood vessels in kidney. Otherwise, the low dose of the treated drugs showed no histopathological alteration and the normal histological structure of the central vein and surrounding hepatocytes in the parenchyma were recorded and the glomeruli and tubules at the cortex were recorded with no toxicological changes. Our results were in agreement with a previous report (Ning et al., 2014).found that the immunohistochemical results showed the kidney function related proteins of IgG, IgM and VEGF were highly expressed when treated with the high dose of AV, whereas the IgA and nephrin were not significantly expressed at the low doses. Podocytes were observed extensively fused in cisplatin group and AV at their high doses. All these changes are considered to be the promising indicators for early

kidney and liver injury, and they are probably involving in injury mechanism by high dose of AV. So, low doses are recommended for further therapeutic studies using the current synthesized platforms.

Kidney injury caused by the high doses of AV is a process induced by subsequent signaling cascades. In the glomeruli, VEGF is continuously expressed and secreted by podocytes to protect the integrity of filtering membrane (Eremina and Quaggin 2010). It was observed that, the expression of VEGF protein was significantly down-regulated in the kidney of rats after a period of AV treatment. In addition, the podocytes were extensively fused in rats injected with AV. The data indicates that the down-regulated VEGF is likely due to the disturbance of glomerular basement membrane. Further decline in VEGF expression was observed in the kidney of rats by higher dose of AV, which might be explained by podocytes apoptosis being induced by inhibition of VEGF activity (Hara et al ., 2006)In this process, the AV may activate alexin cascade, causing the formation of cell membrane attack complex and triggering cytolytic toxicity (Zhang and Huang 2012)AV caused podocytes damage may mediated by down-regulation of a member of immunoglobulin (Ig) superfamily-slit diaphragm nephrin (Sugimoto et al ., 2003)

Our histology results indicated that there were no significant changes in nephrin expression levels in the kidney biopsy specimens of treated rats. The expression of nephrin was not always consistent in other kidney injury (Bignami et al., 2013).These discrepant results may be explained by the differences in kidney injury degree and the methods in detecting protein expression. Patients who suffered from chemotherapy of anti-VEGF lead to proteinuria indicating injury of the glomerular filtration barrier (Eremina et al., 2008).Another immunoglobulin superfamilies, IgG and IgM were found higher deposited in the high dose AV treated groups. Accordingly, it was concluded that the AV-induced proteinuria was related to immunoglobulin deposition.

CONCLUSION

We concluded that AV and CR increase the risk of injury in glomerular filtration barrier and hepatocytes in their high doses, but their nano-capsules may overcome this noted risk using their lowest doses. Intriguingly, drug-drug combinatorial therapeutic strategy may reduce the noticed side effects by inducing beneficial synergistic effect between both drugs (Eskander et al., 2012).

CONFLICT OF INTEREST

The authors declared that present study was performed in absence of any conflict of interest.

ACKNOWLEGEMENT

This work was supported by the National Research Centre Grant (No: 11010333) to the principle investigator Dr. Abd-Rabou. The study protocol followed the guidelines approved by the Ethical Committee of the Medical Research of the National Research Centre (Approval No. 16/ 281).

AUTHOR CONTRIBUTIONS

AAA-R hypothesized the idea of the study, designed and planned the work, gained the fund, synthesized and characterized the nanoparticles, performed hematological and histopathological investigations, glucose profiling, performed data analysis, and wrote the paper. SHM and SEK arranged and dealt with animal experiments (acute and chronic toxicity), animal treatments, tissue and sample collection, and performed the biochemical assays. HHA designed and managed the work, performed data analysis, and revised the paper. MSK contributed in tissue and sample collection, hematology and glucose experiments. All authors read, revised, and approved the final version.

REFERENCES

A.O.A.C.(1995) Official Methods of Analysis, 16th ed, Association of Official Analysis, Washington, DC.

Abd-Rabou AA, Abdalla AM, Ali NA, Zoheir KM. (2017) Moringaoleifera Root Induces Cancer Apoptosis more Effectively than Leave Nanocomposites and Its Free Counterpart. Asian Pac J Cancer Prev. 18(8):2141-2149.

Abd-Rabou AA (2017) Calcium, a Cell Cycle Commander, Drives Colon Cancer Cell Diffpoptosis. Ind J Clin Biochem DOI 10.1007/s12291-016-0562-0

Abd-Rabou AA, Ahmed HH, Kishta MS (2019)

Synthesis, characterization, and *in vivo* immunomodulation of ccr2 and vascular endothelial growth factor antagonists-loaded pegylated nanoparticles. Asian J Pharm Clin Res, 12(1): 275-285.

Abd-Rabou AA, Ahmed HH. (2017) CS-PEG decorated PLGA nano-prototype for delivery of bioactive compounds: A novel approach for induction of apoptosis in HepG2 cell line. Advances in Medical Sciences. 62(2):357–367.

Abd-Rabou AA, Bharali DJ, Mousa SA. (2018) Taribavirin and 5-Fluorouracil-loaded Pegylated-lipid Nanoparticle Synthesis, p38 Docking, and Antiproliferative Effects on MCF-7 Breast Cancer. Pharmaceutical Research. 35(4):76.

Abd-Rabou AA, Edris A. (2017) Evaluation of the Antiproliferative Activity of Some Nanoparticulate Essential Oils Formulated in Microemulsion on Selected Human Carcinoma Cell Lines. Current Clinical Pharmacology. 12(4): 231-244.

Abd-Rabou AA, Zoheir KMA, Kishta MS, Shalby AB, Ezzo MI (2016) Nano-micelle of moringaoleifera seed oil triggers mitochondrial cancer cell apoptosis. Asian Pac J Cancer Prev 17(11):4929–4933.

Aleksunes LM, Augustine LM, Scheffer GL, Cherrington NJ, Manautou JE.(2008) Renal xenobiotic transporters are differentially expressed in mice following cisplatin treatment. Toxicology. 250(2-3):82–88.

Arao T, Matsumoto KM, Nishio KT. (2011). Therapy for Cancer: Anti-cancer Drugs Targeting Growth-Factor Signaling Molecules. Biol Pharm Bull. 34(12):1789–1793.

B.-Z. Qian, J. Li, H. Zhang et al., (2011) "CCL2 recruits inflammatory monocytes to facilitate breast-tumour metastasis," Nature. 475(7355): 222–225.

Banchroft JD, Stevens A, Turner DR. (1996) THEORY AND PRACTICE OF HISTOLOGICAL TECHNIQUES. Fourth Ed. ChurchilLivingstone ,New York , London , San Francisco, Tokyo.

Bao W, Liu R, Wang Y, Wang F, Xia G, Zhang H, Li X, Yin H and Chen B. (2015) PLGA-PLL-PEG-Tf-based targeted nanoparticles drug delivery system enhance antitumor efficacy via intrinsic apoptosis pathway. Int J Nanomedicine. 12(10):557-566.

Baty F, Rothschild S, Fruh M, et al (2013) EGFR exon-level biomarkers of the response to bevacizumab/erlotinib in non-small cell lung cancer. PLoS One.;8(9): 72966.

Bellomo R, Kellum JA, Ronco C. (2004) Defining acute renal failure: physiological principles. Intensive Care Med. 30(1):33–37.

Bignami E, Casamassima N, Frati E, Lanzani C, Corno L, Alferi O, Gottlieb S, Simonini M, Shah KB, Mizzi A. (2013) Preoperative endogenous ouabain predicts acute kidney injury in cardiac surgery patients. Crit Care Med.41(3):744-755.

Bottsford-Miller JN, Coleman RL, Sood AK. (2012) Resistance and escape from antiangiogenesis therapy: clinical implications and future strategies. Journal of Clinical Oncology. 30 (32): 4026–4034.

British Medical Association. (2015) British national formulary : BNF 69 (69 ed.) p. 597.

Burtis A et al., Tietz (1999)Textbook of Clinical Chemistry, 3rd ed AACC.

Chae SY, Kim TH, Park K, Jin H, Son S, Lee S, et al., (2010) Improved antitumor activity and tumor targeting of NH(2)-terminal-specific PEGylated tumor necrosis factor-related apoptosis-inducing ligand. Mol Cancer. 9(6):1719-1729.

Conti I, Rollins BJ. (2004) CCL2 (monocyte chemoattractant protein-1) and cancer. Semin Cancer Biol. 14(3): 149- 154.

Duvvuri S, Janoria KG, Pal D, Mitra AK. (2007) Controlled delivery of ganciclovir to the retina with drug-loaded Poly(D,L-lactide-coglycolide)(PLGA) microspheres dispersed in PLGA-PEG-PLGAgel: a novel intravitreal delivery system for the treatment ofcytomegalovirus retinitis. J OculPharmacolTher. 23(3): 264-74.

Eremina V, Jefferson JA, Kowalewska J, Hochster H, Haas M, Weisstuch J, Richardson C, Kopp JB, Kabir MG, Backx PH. (2008) VEGF inhibition and renal thrombotic microangiopathy. N Engl J Med. 358(11) :1129–1136.

Eremina V, Quaggin SE. (2010)Biology of anti-angiogenic therapy-induced thrombotic microangiopathy. SeminNephrol. 30(6):582–90.

Eskander EF, Abd-Rabou AA, Yahya SMM, et al (2012) Does interferon and ribavirin combination therapy ameliorate growth hormone deficiency in HCV genotype-4 infected patients? Clin. Biochem. 45: 3-6.

Fang WB, Jokar I, Zou A, Lambert D, Dendukuri P, Cheng N. (2012) CCL2/CCR2 chemokine signaling coordinates survival and motility of

breast cancer cells through Smad3 protein- and p42/44 mitogen-activated protein kinase (MAPK)- dependent mechanisms. J Biol Chem. 287: 36593- 36608.

Ferrara N, Hillan K, Novotny W. (2005) Bevacizumab (Avastin), a humanized anti-VEGF monoclonal antibody for cancer therapy. BiochemBiophys Res Commun. 333(2): 328-335.

Folkman J. (1971) Tumor angiogenesis: therapeutic implications. N Engl J Med. 285(21):1182-1186.

Fridlender ZG, Buchlis G, Kapoor V, et al.,(2010) "CCL2 blockade augments cancer immunotherapy," Cancer Researchearch. 70(1) 109–118.

Giordano GG, Chevez B, Refojo MF, Garcia CA. (1995) Biodegradation and tissue reaction to intravitreousbiodegradablepoly(DL-lactic-co-glycolic)acid microspheres. Curr Eye Res., 14(9): 761-768.

Guan F, Villegas G, Teichman J, Mundel P, Tufro A.(2006) Autocrine VEGF-A system in podocytes regulates podocin and its interaction with CD2AP. Am J Physiol Renal Physiol.291(2):422–428.

Hao Y, Patel A, Liu W, Krishna R, Sabates NR, Mitra AK. (2009) Preparation and characterization of bevacizumab (avastin) nanoparticles for the treatment of age related macular degeneration. American Association of Pharmaceutical Scientists (AAPS) Annual Meeting and Exposition, Los Angeles, California, U.S.A. November, 2009. Available from http://www.aapsj.org/abstracts/AM_2009/AAPS2009-002539.PDF

Hara A, Wada T, Furuichi K, Sakai N, Kawachi H, Shimizu F, Shibuya M, Matsushima K, Yokoyama H, Egashira K. (2006) Blockade of VEGF accelerates proteinuria, via decrease in nephrin expression in rat crescentic glomerulonephritis. Kidney Int. 69(11):1986–1995.

Herget RS, Marggraf G, Hüsing J, Göring F, Pietruck F, Janssen O, Philipp T, Kribben A. (2004) Early detection of acute renal failure by serum cystatin C. Kidney Int.66(3):1115–22.

Hu JY, Meng XC, Han J, Xiang F, Fang YD, Wu J, Peng YZ, Wu YZ, Huang YS, Luo QZ. (2012) Relation between proteinuria and acute kidney injury in patients with severe burns. CritCare.16(5):R172.

International Drug Price Indicator Guide. (2016) "Bevacizumab". Retrieved 8 December 2016.

Izzedine H, Massard C, Spano JP, Goldwasser FO, Khayat D, Soria JC. (2010) VEGF signalling inhibition-induced proteinuria: Mechanisms, significance and management. Eur J Cancer. 46(2): 439–448.

Kaplan A et al., (1984) ClinChemThe C.V. Mosby Co. St Louis. Toronto. Princeton; 1257-1260 and 437and 418.

Kim KJ, Li B, Winer J, Armanini M, Gillett N, Phillips HS, Ferrara N.(1993) Inhibition of vascular endothelial growth factor-induced angiogenesis suppresses tumour growth *in vivo*. Nature. 362(6423):841–844.

Li F, Hurley, Liu Y, Leonard B and Griffith M. (2012) Controlled Release of Bevacizumab Through Nanospheres for Extended Treatment of Age-Related Macular Degeneration. The Open Ophthalmology Journal. 6: 54-58.

Liu Z, Vunjak NG. (2016) "Modeling tumor microenvironments using custom-designed biomaterial scaffolds," CurrOpinChem Eng., 16:94-105.

Machado FG, Kuriki PS, Fujihara CK, Fanelli C, Arias SC, Malheiros DM, Camara NO, Zatz R. (2012) Chronic VEGF blockade worsens glomerular injury in the remnant kidney model. PLoS7(6): e39580.

Marko R, Manuela C, Martin S, Daniela S, Reiner Z, Maya S, Gerd B, Lubor B. (2015) Targeted delivery of CCR2 antagonist to activated pulmonary endothelium prevents metastasis. Journal of Controlled Release. 220: 341–347

Mayer G. (2011) Capillary rarefaction, hypoxia, VEGF and angiogenesis in chronic renal disease. Nephrol Dial Transplant.26(4):1132–1137.

Mitchell LA, Hansen RJ, Beaupre AJ, Gustafson DL, Dow SW.(2013) Optimized dosing of a CCR2 antagonist for amplification of vaccine immunity. IntImmunopharmacol. 15(2):357-363.

Monti P, Leone BE, Marchesi F, Balzano G, Zerbi A, Scaltrini F, Pasquali C, Calori G, Pessi F, Sperti C, Di Carlo V, Allavena P, Piemonti L. (2003) The CC chemokine MCP-1/CCL2 in pancreatic cancer progression: regulation of expression and potential mechanisms of antimalignant activity. Cancer Res. 63(21): 7451-7461.

Murray R. (1984)Alanine aminotransferase. Kaplan A et al., ClinChemThe C.V. Mosby Co. St Louis. Toronto. Princeton. 1088-1090.

Ning Z ,Qunhong X, Ming W, et al (2014)

Mechanism of kidney injury caused by bevacizumab in rats.Int J ClinExpPathol. 7(12): 8675–8683.

Pan CK, Durairaj C, Kompella UB, et al., (2011) Comparison of long acting bevacizumab formulations in the treatment of choroidal neovascularization in a rat model. J OculPharmacolTher; 27(3): 219-24.

Park JH, Lee S, Kim JH, et al., (2008) Polymeric nanomedicine for cancer therapy. ProgPolym Sci. 33(1): 113-137.

Pellé G, Shweke N, Van Huyen JPD, et al (2011) Systemic and kidney toxicity of intraocular administration of vascular endothelial growth factor inhibitors. Am J Kidney Dis. 57(5):756–759.

Salcedo R, Ponce ML, Young HA, Wasserman K, Ward JM, Kleinman HK, Oppenheim JJ, Murphy WJ. (2000) Human endothelial cells express CCR2 and respond to MCP- 1: direct role of MCP-1 in angiogenesis and tumor progression. Blood. 96(1): 34-40.

Sato S, Itamochi H. (2012) Bevacizumab and ovarian cancer. CurrOpinObstet Gynecol. 24(1):8–13.

Singh AP, Junemann A, Muthuraman A, Jaggi AS, Singh N, Grover K, Dhawan R. (2012) Animal models of acute renal failure. PharmacolRep.64(1):31–44.

Sugimoto H, Hamano Y, Charytan D, Cosgrove D, Kieran M, Sudhakar A, Kalluri R. (2003) Neutralization of circulating vascular endothelial growth factor (VEGF) by anti-vegf antibodies and soluble VEGF receptor 1 (sFlt-1) induces proteinuria. J Biol Chem. 278(15):12605–8.

Tahara K., Furukawa S, Yamamoto H and Kawashima Y. (2010) Hybrid-modified poly(D,L-lactide-co-glycolide) nanospheres for a novel cellular drug delivery system. Int J Pharm. 392(1-2):311–313.

Tangirala RK, Murao K, Quehenberger O. (1997)Regulation of expression of the human monocyte chemotactic protein-1 receptor (hCCR2) by cytokines. J Biol Chem. 272(12): 8050-8056.

The American Society of Health-System Pharmacists. (2016). "Bevacizumab". Archived from the original on 20 December 2016.

Tietz N W et al.,(1995) Clinical Guide to Laboratory Tests, 3rd ed AACC.

Umano M, Uechi K, Uriuda T, et al., (2011): Tumor accumulation of epsilon-poly-lysines-based polyamines conjugated with boron clusters. ApplRadiatIsot. 69(12):1765–1767.

Wenger C. et al., (1984) Alkaline phosphatase. Kaplan A et al., ClinChemThe C.V. Mosby Co. St Louis. Toronto. Princeton. 1094-1098.

Wolf MJ, Hoos A, Bauer J, Boettcher S, Knust M, Weber A, Simonavicius N, Schneider C, Lang M, Sturzl M, Croner RS, Konrad A, Manz MG, et al.,(2012) Endothelial CCR2 signaling induced by colon carcinoma cells enables extravasation via the JAK2-Stat5 and p38MAPK pathway. Cancer Cell. 22(1): 91-105.

World Health Organization. (2013)"WHO Model List of EssentialMedicines"from the original on 23 April 2014.

World Health Organization.(2015) "WHO Model List of Essential Medicines (19th List)" from the original on 13 December 2016.

Xu J, Wang Y, Li Y, et al., (2007) Inhibitory Efficacy of IntravitrealDexamethasone Acetate-Loaded PLGA Nanoparticles onChoroidal Neovascularization in a Laser-Induced Rat Model. JOculPharmacolTher. 23(6): 527-39.

Zachariae CO, Anderson AO, Thompson HL, Appella E, Mantovani A, Oppenheim JJ, Matsushima K.(1990) Properties of monocyte chemotactic and activating factor (MCAF) purified from a human fibrosarcoma cell line. J Exp Med. 171(6): 2177-2182.

Zhang A, Huang S. (2012) Progress in pathogenesis of proteinuria. Int J Nephrol. 314251.

Zhang J, Lu Y, Pienta KJ. (2010) Multiple roles of chemokine (C-C motif) ligand 2 in promoting prostate cancer growth. J Natl Cancer Inst. 102(8):522-528.

Zhao J, Li H, Wang M. (2009) Acute renal failure in a patient receiving anti-VEGF therapy for advanced non-small cell lung cancer. J Thorac Oncol.4(9):1185–1187.

Zhu X, Wu S, Dahut WL, (2007) Parikh CR. Risks of proteinuria and hypertension with bevacizumab, an antibody against vascular endothelial growth factor: systematic review and meta-analysis. Am J Kidney Dis. 49(2):186–193.

Zoheir KMA, Abd-Rabou AA, Harisa GI, et al (2015) Gene expression of IQGAPs and Ras families in an experimental mouse model for hepatocellular carcinoma: A mechanistic study of cancer progression. Int J Clin Exp Pathol 8(8):8821-883.